

Overview of recent physics results from MAST

Andrew Kirk
and the MAST team

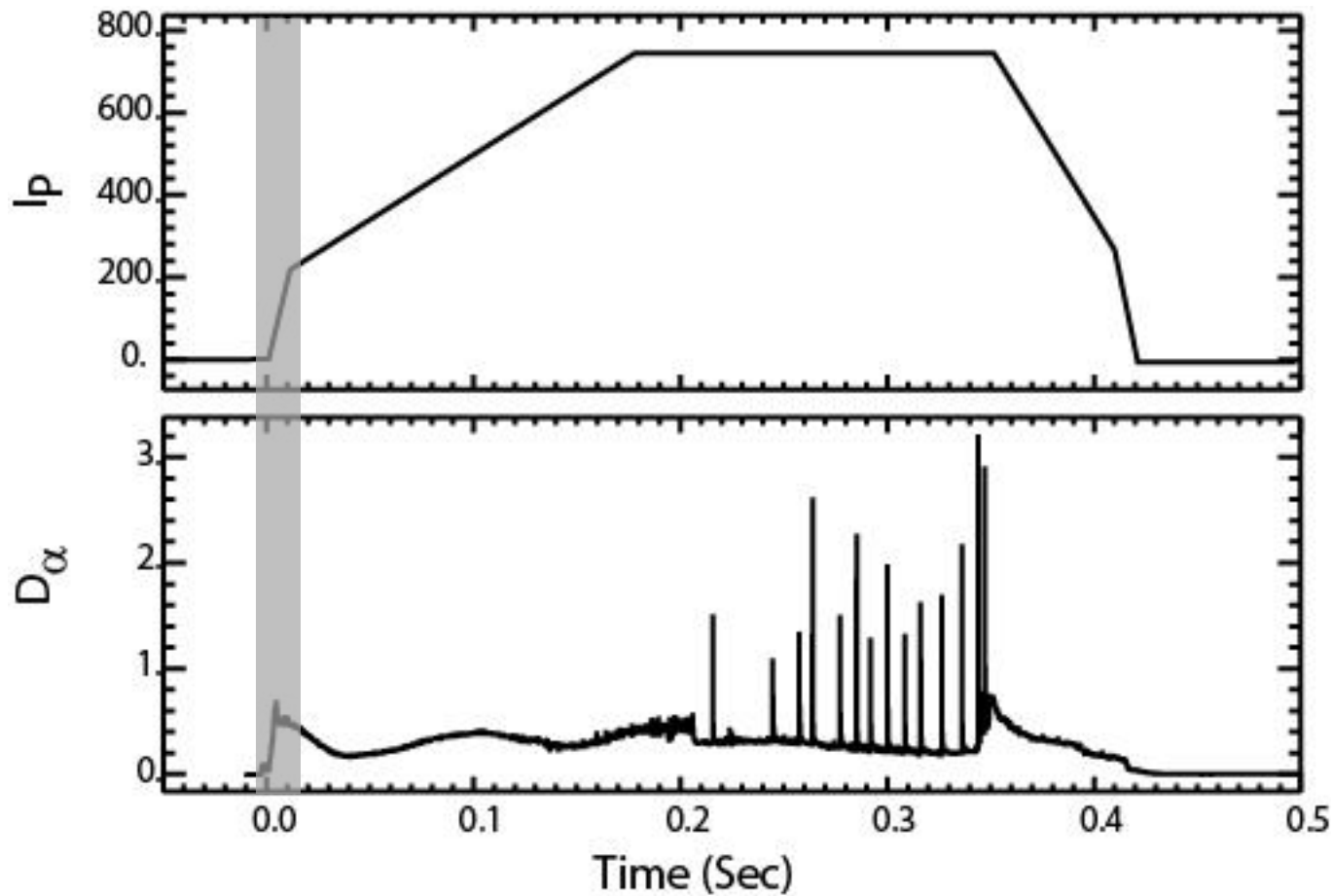
Presented at the IAEA FEC, Kyoto
October 2016

Overview of recent physics results from MAST

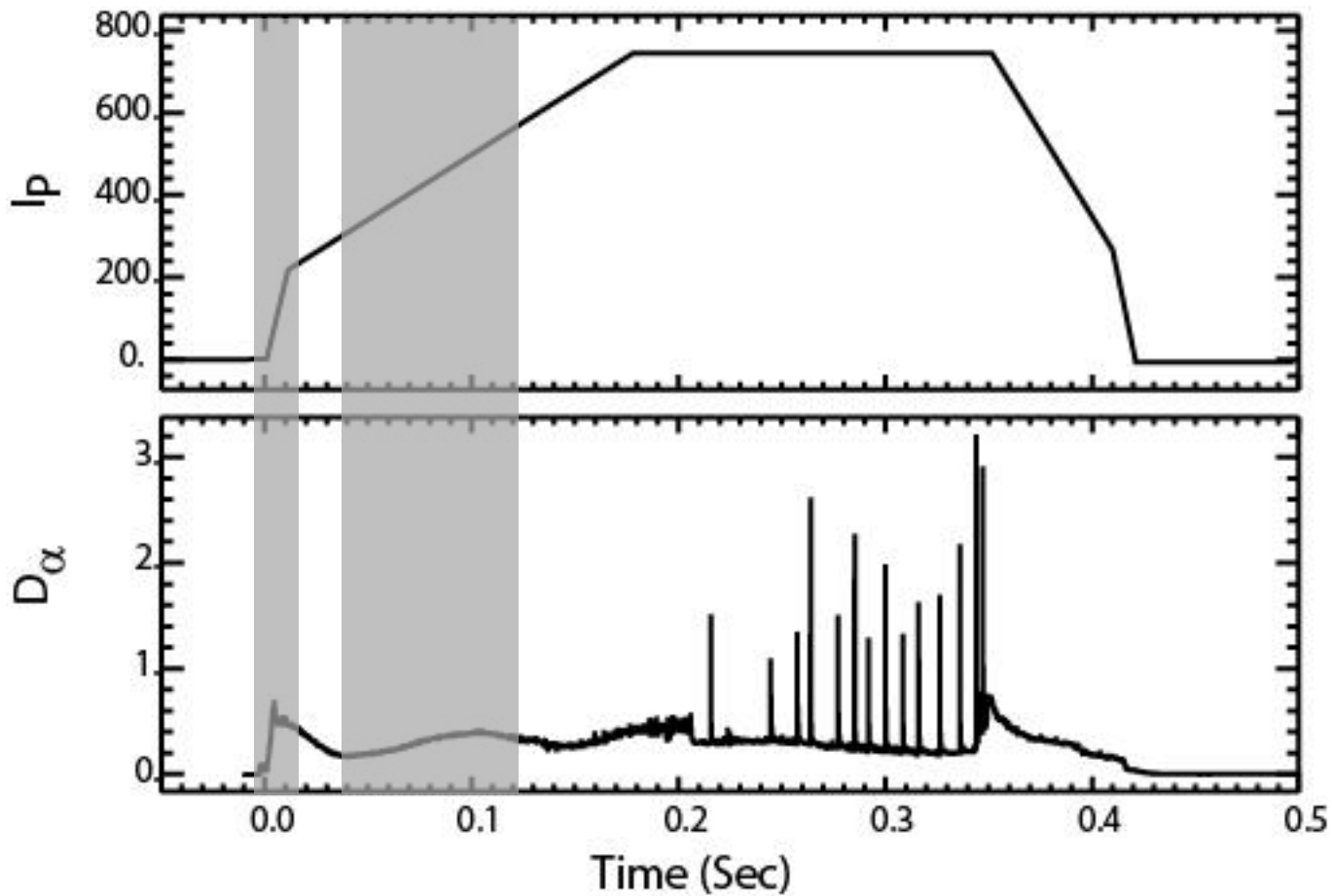
Andrew Kirk
On behalf of



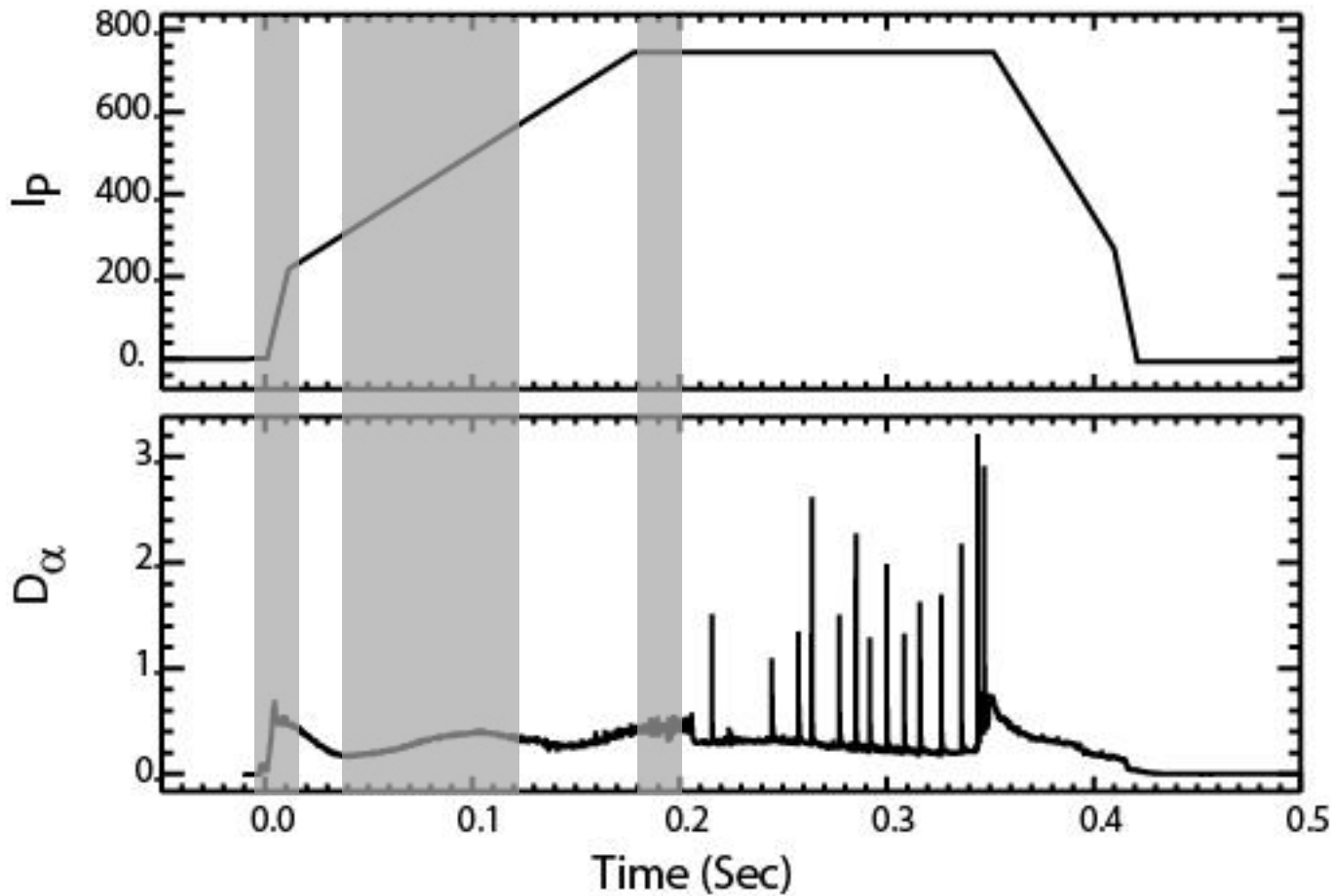
Start-up



Start-up
Current
Ramp



Start-up
Current
Ramp L-mode

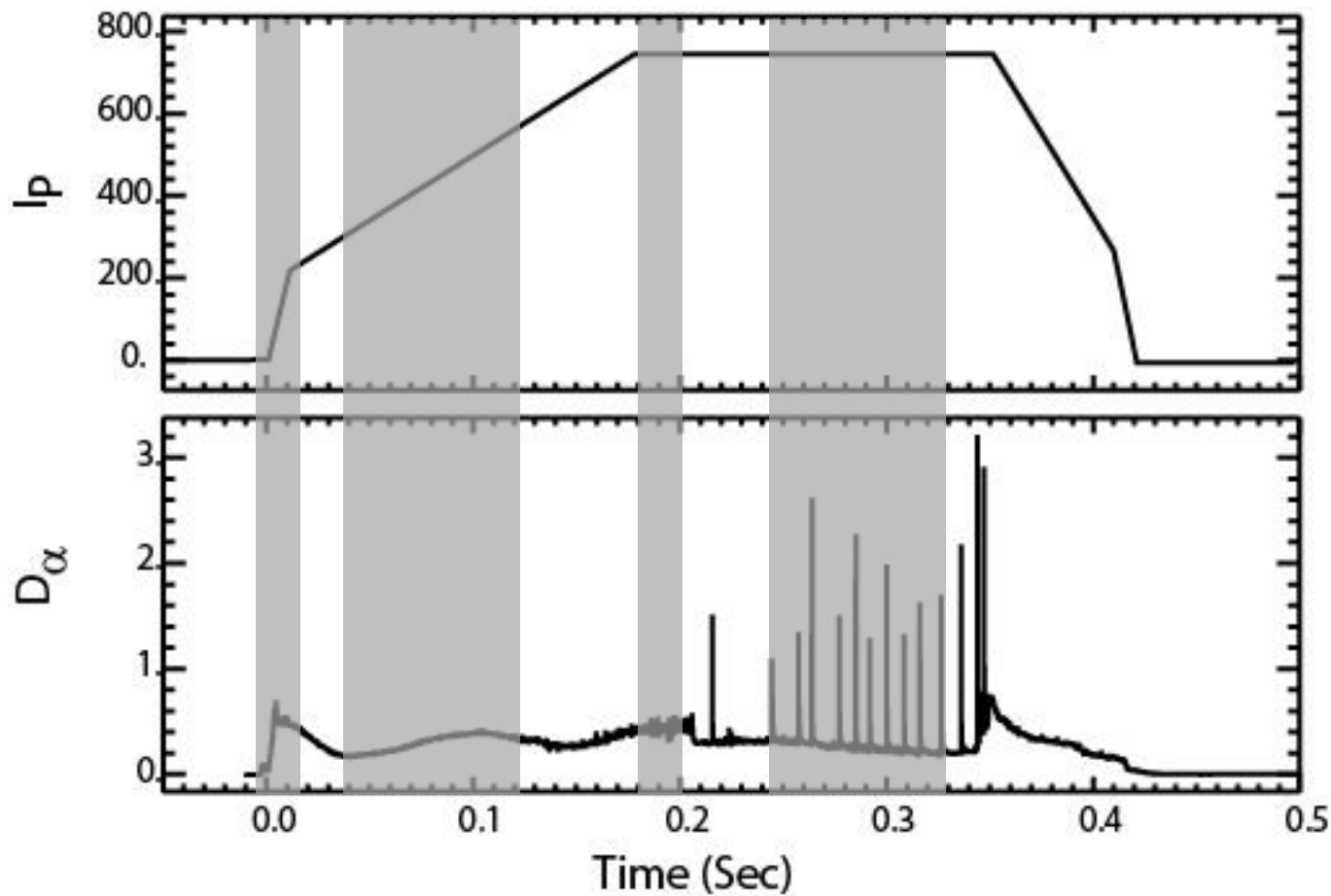


Start-up

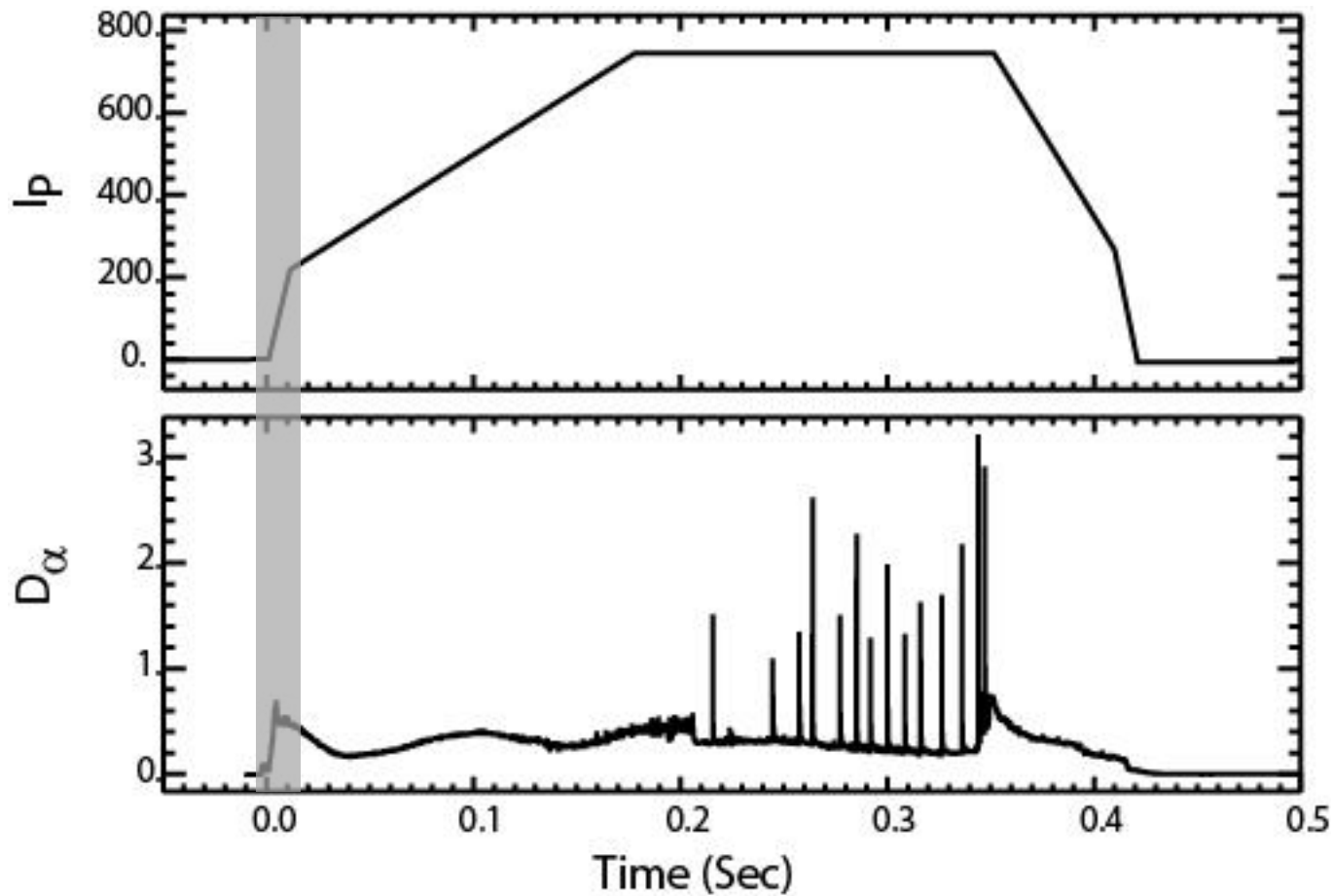
Current
Ramp

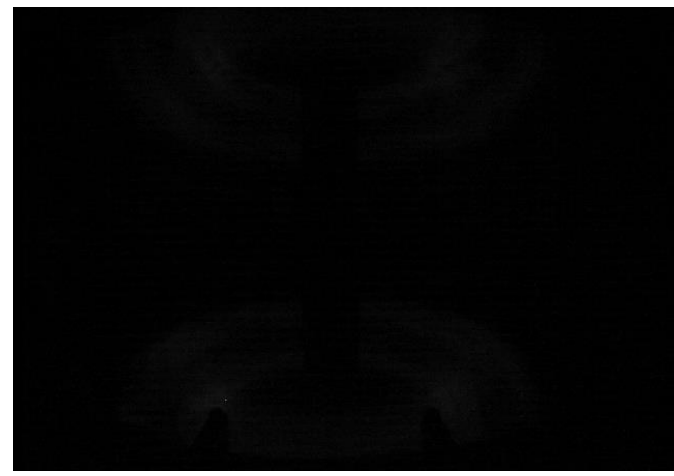
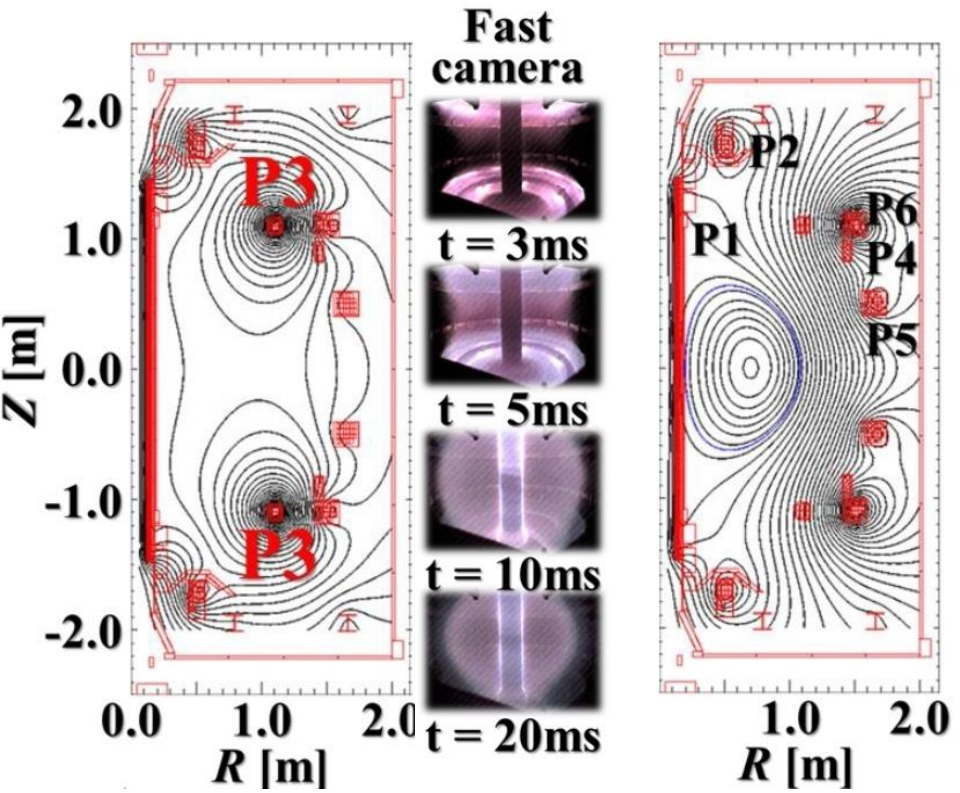
L-mode

H-mode



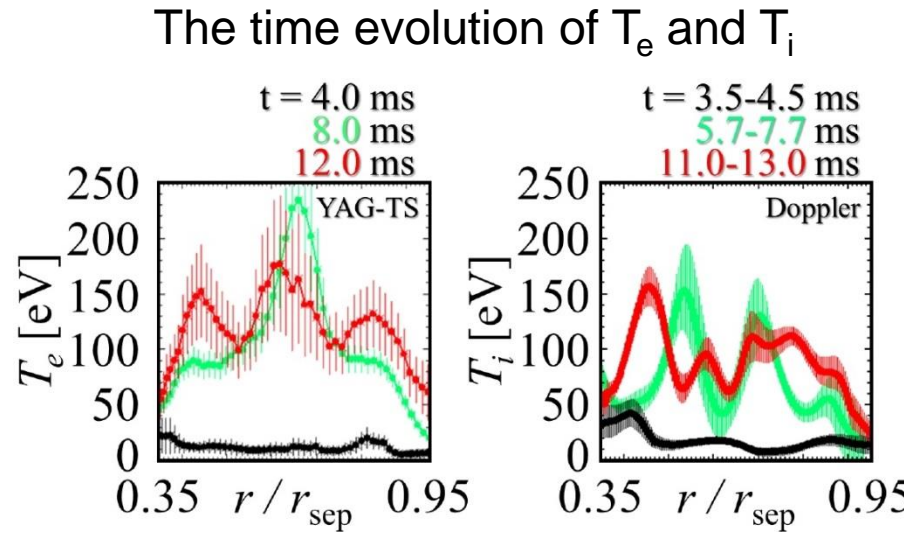
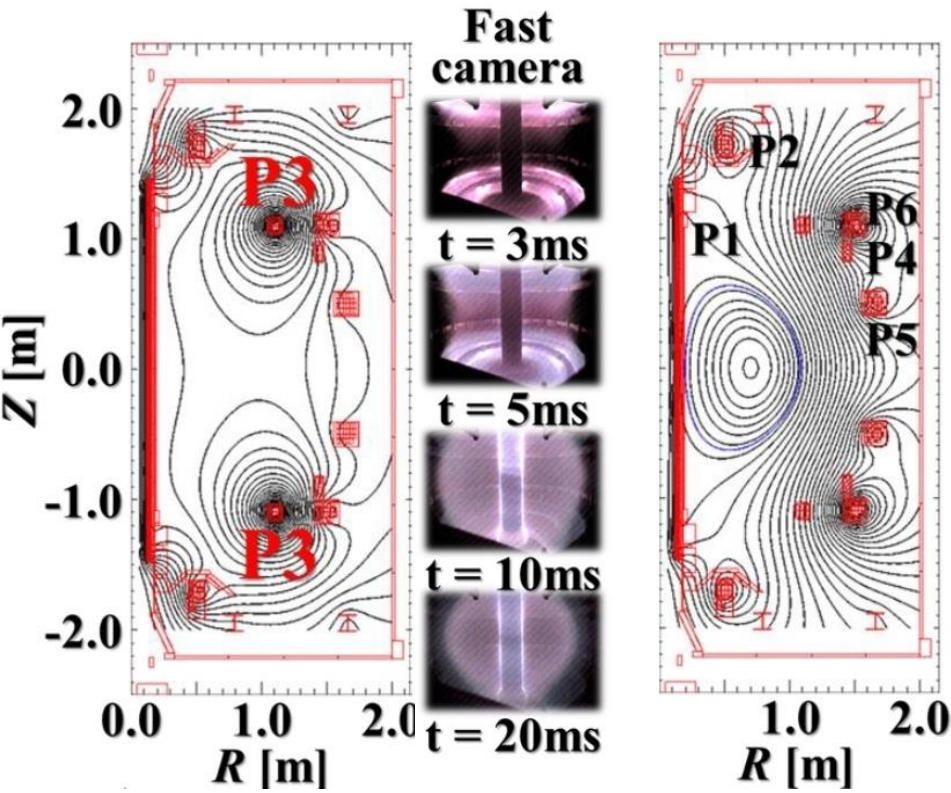
Start-up





Effect of reconnection on ion heating

H. Tanabe et al., 115, 215004, PRL, (2015)

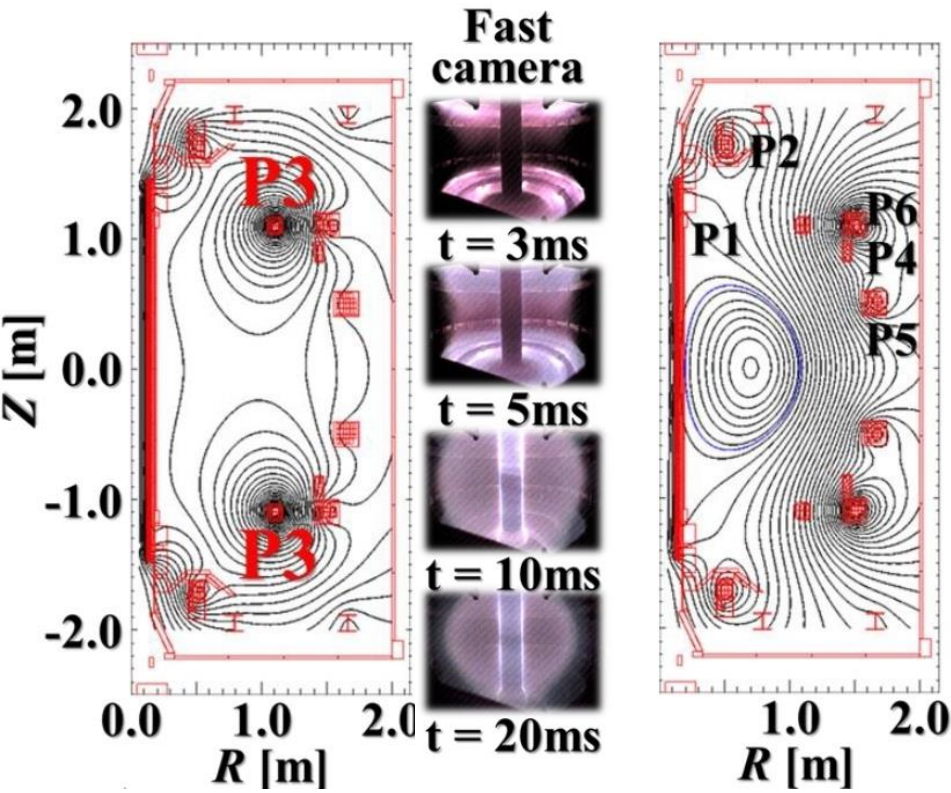


T_e Peaks at the X-point

T_i increases downstream

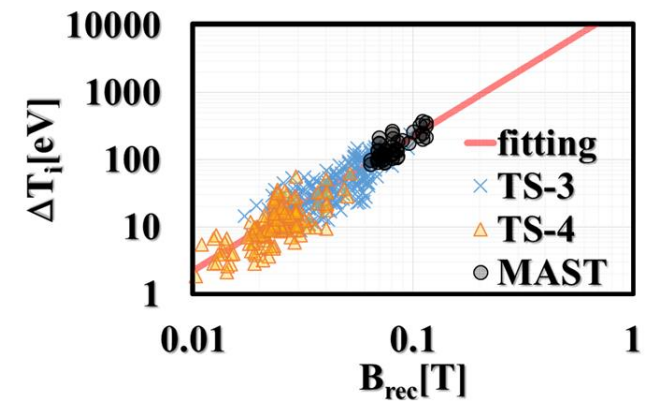
Modelling with HIFI code shows this is due to magnetic energy being converted to thermal energy

P. Browning et al., PPCF 58, 014041 (2016)



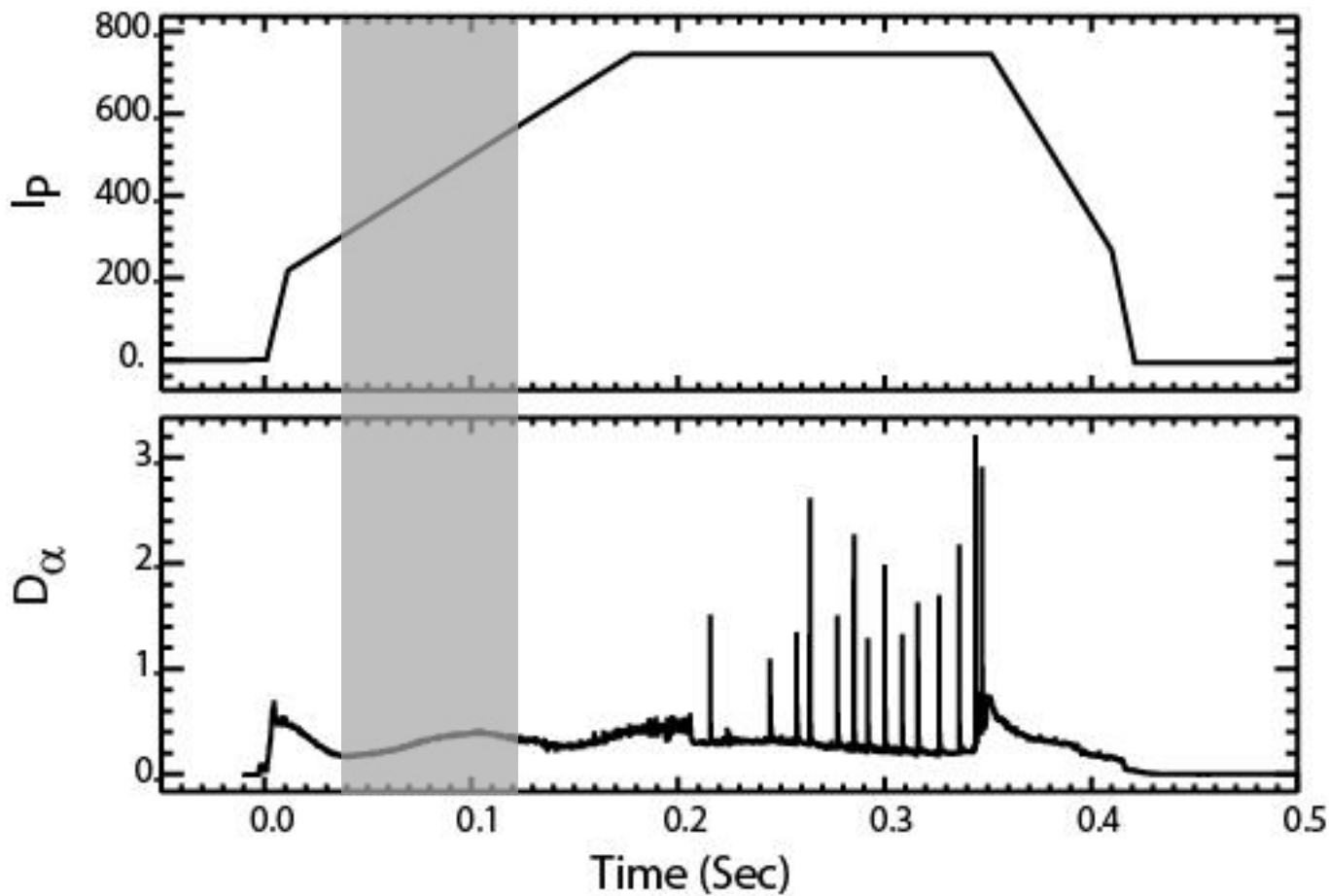
The bulk ion temperature rises due to the reconnection process

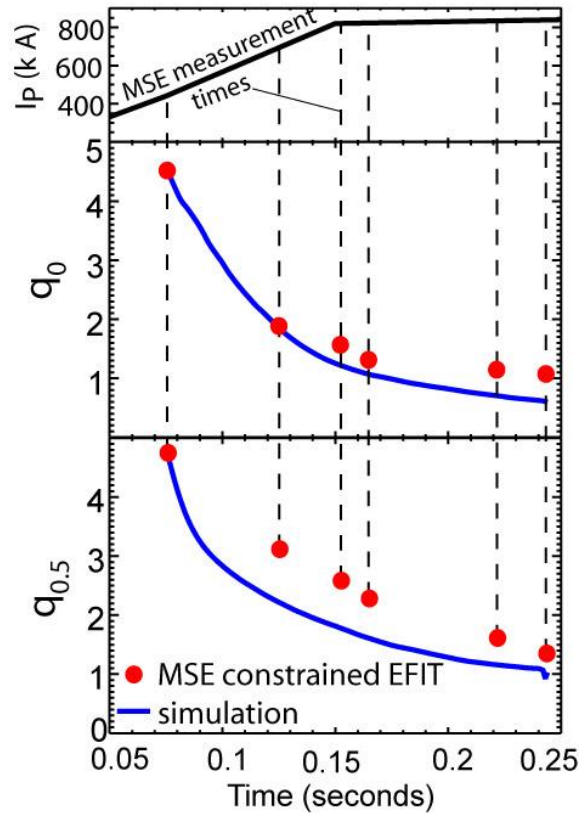
$$\Delta T_i \propto B_{rec}^2$$



EX/P4-32 H. Tanabe

Current Ramp





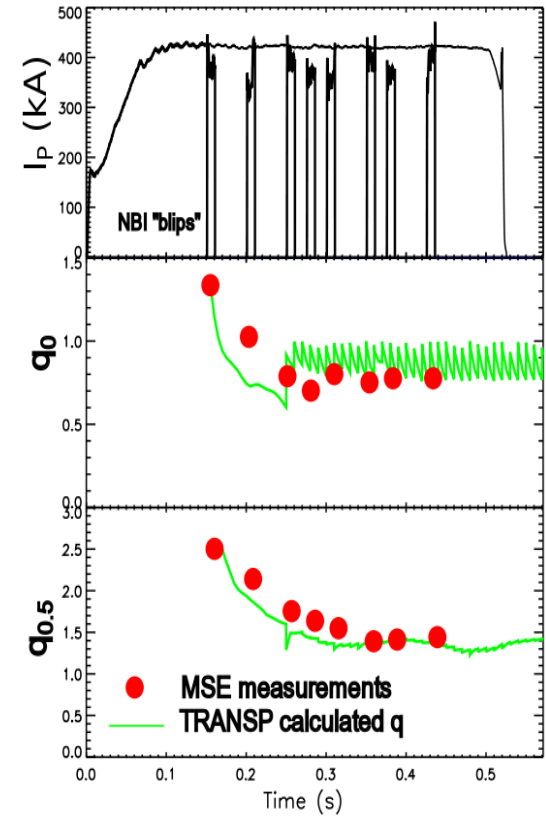
Previous experiments on MAST have shown that:

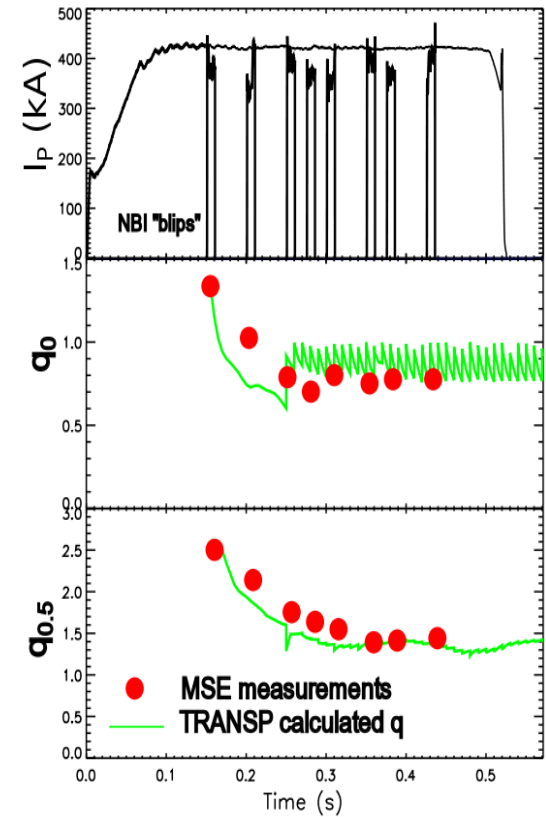
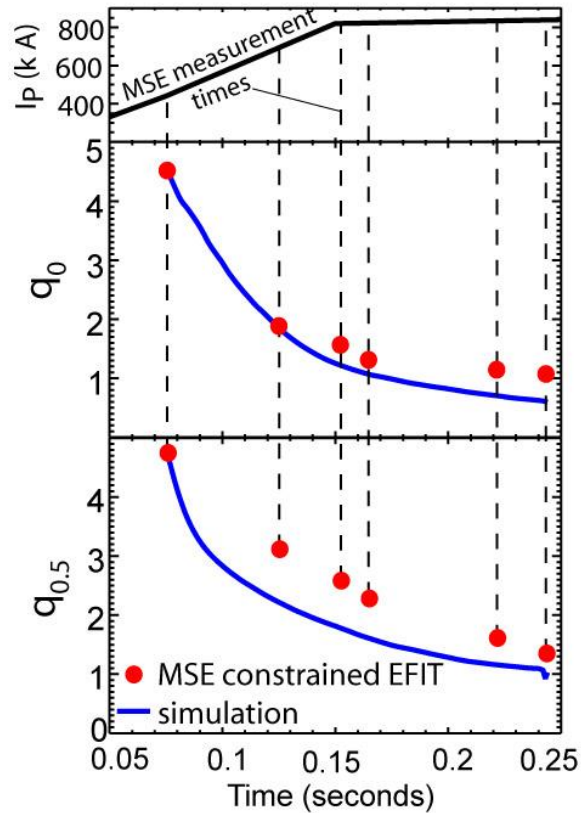
- In both I_p ramp-up and I_p ramp-down **the current diffusion is not well modelled by TRANSP**
- Current diffusion in model is faster than observed in experiments

NBI “notcher” used to take Motional Stark Effect (MSE) snapshots of q-profile

Experiments repeated in
 the flat top period

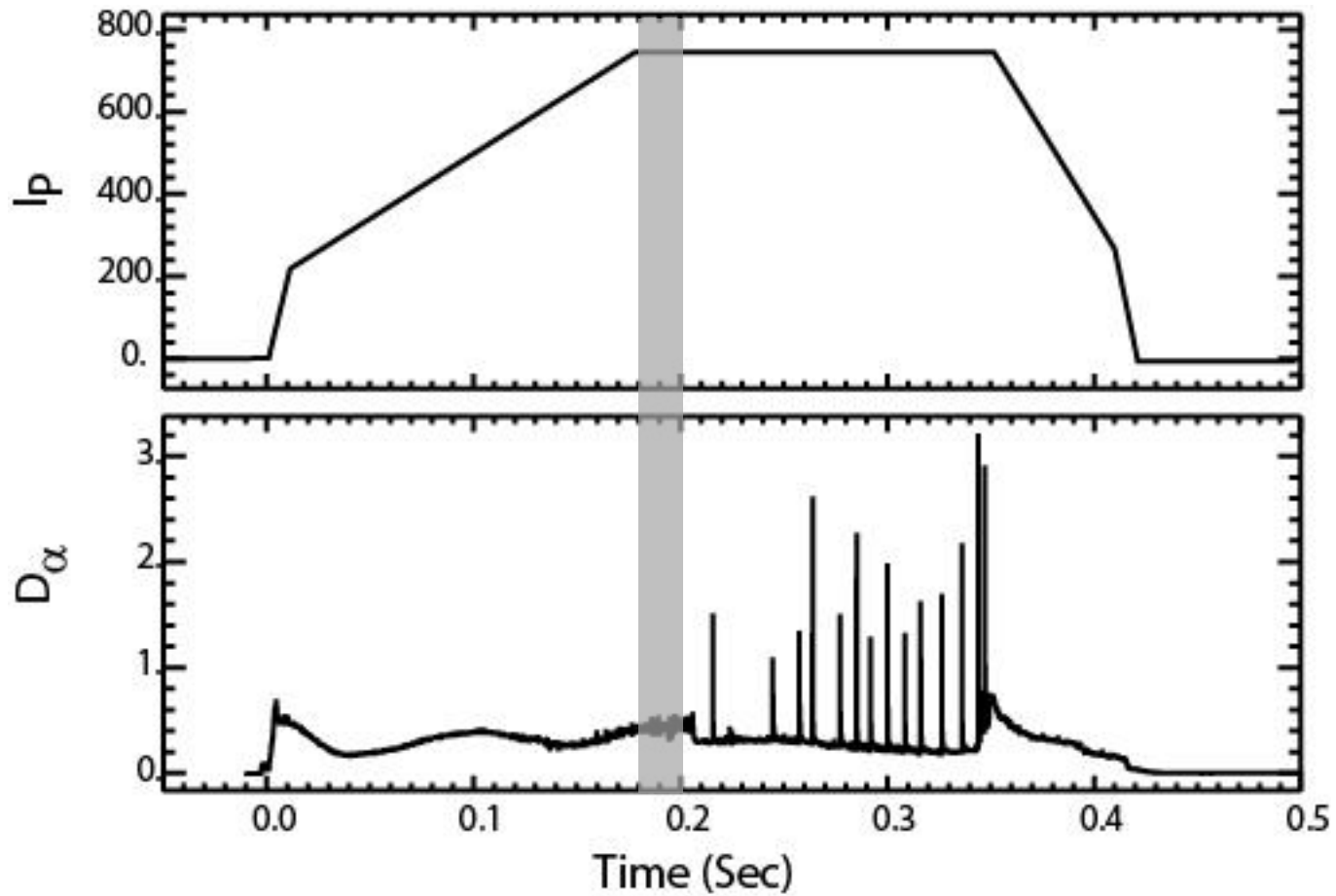
- q-profile match is achieved ~200ms into the flat top using neoclassical resistivity and a sawtooth model.





Conclusion: Our fundamental understanding of current diffusion appears correct but modelling does not accurately reproduce results during the ohmic current ramp

L-mode



SOL transport

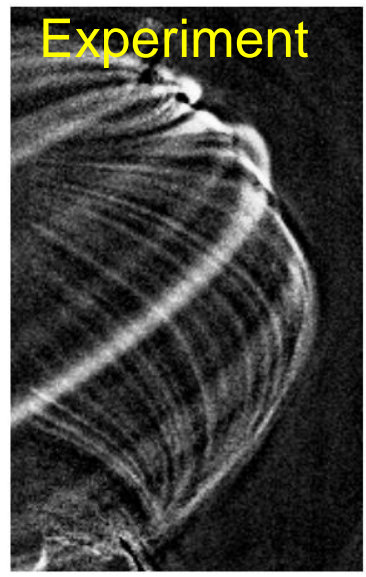
Core transport

SOL transport

Core transport

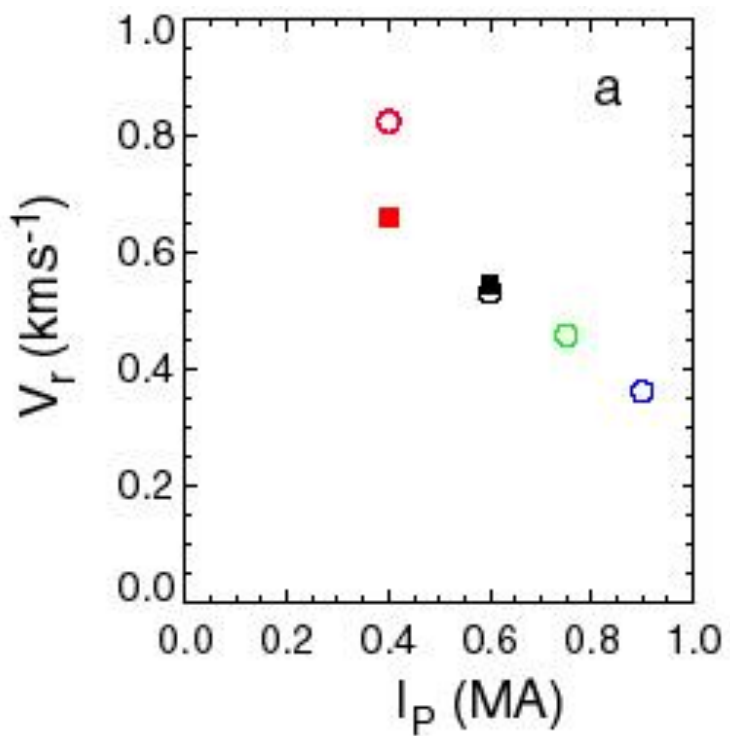
- Filament size and motion measured using fast visual imaging and a variety of probes
- Modelling has been performed using a 3D turbulence code (STORM), which has been able to reproduce most of the filamentary dynamics

STORM – 3D drift wave electrostatic module of BOUT++
Militello et al. PPCF 2016

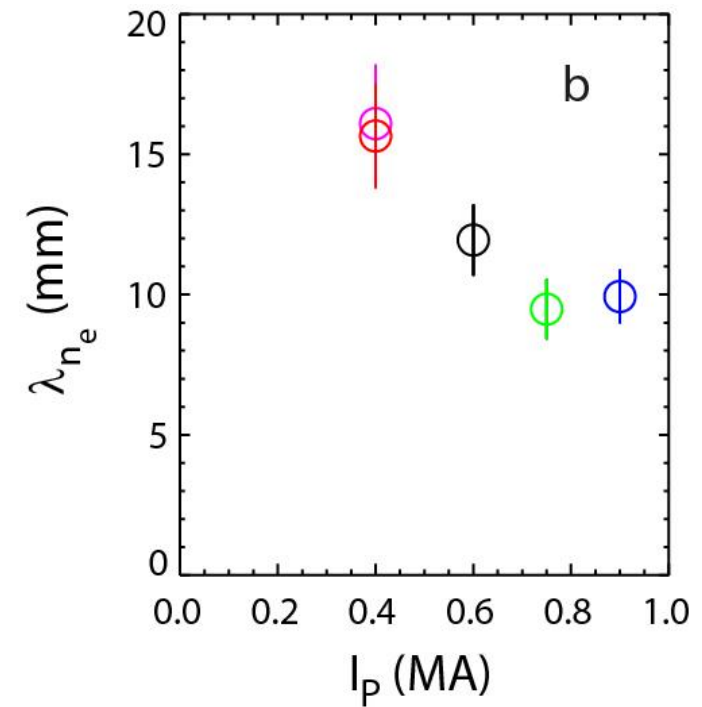


EX/P4-31 F. Militello

- Mid-plane radial velocity of L-mode filaments depends on plasma current [A. Kirk et al, PPCF 2016]

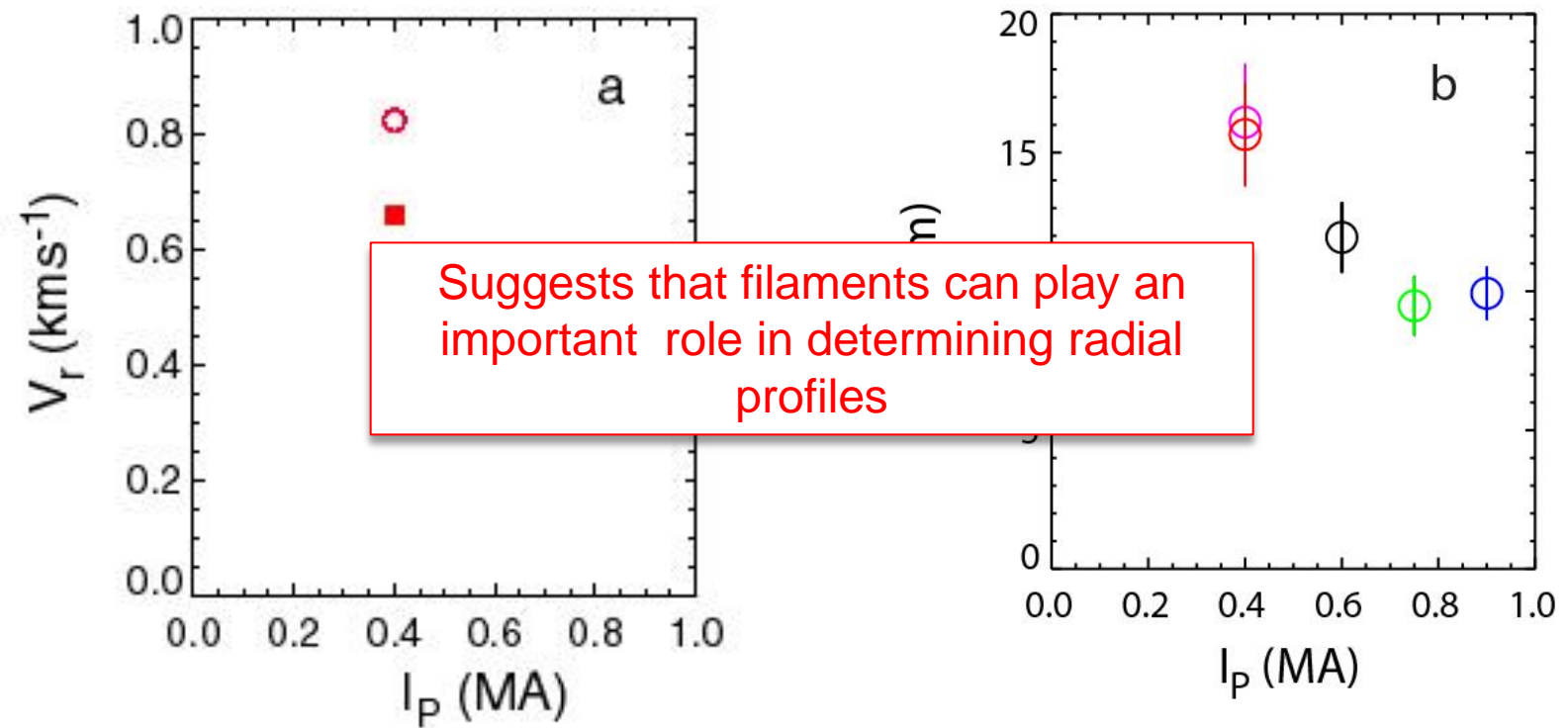


Radial velocity decreases with increasing plasma current



56% reduction in radial velocity consistent with ~60% reduction in density e-folding length at target

- Mid-plane radial velocity of L-mode filaments depends on plasma current [A. Kirk et al, PPCF 2016]



Radial velocity decreases with increasing plasma current

56% reduction in radial velocity consistent with ~60% reduction in density e-folding length at target

- Filament modelling using STORM at constant pressure, the electron temperature significantly affects filament dynamics

$$\delta T / T \ll \delta n / n$$

Propagate further radially

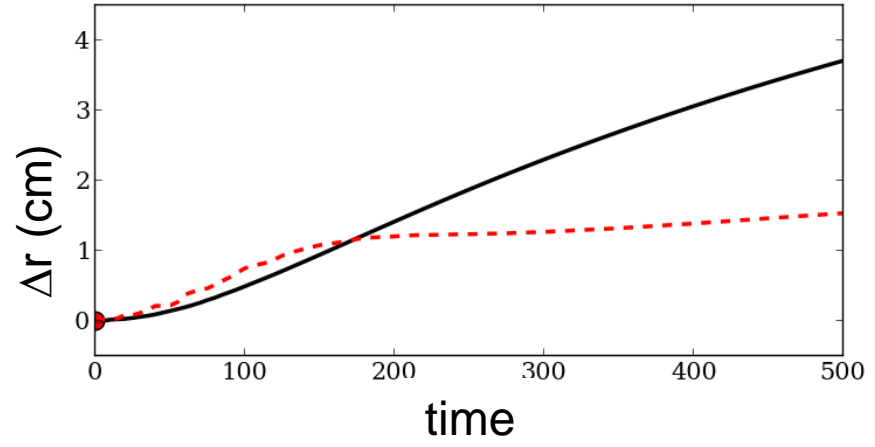
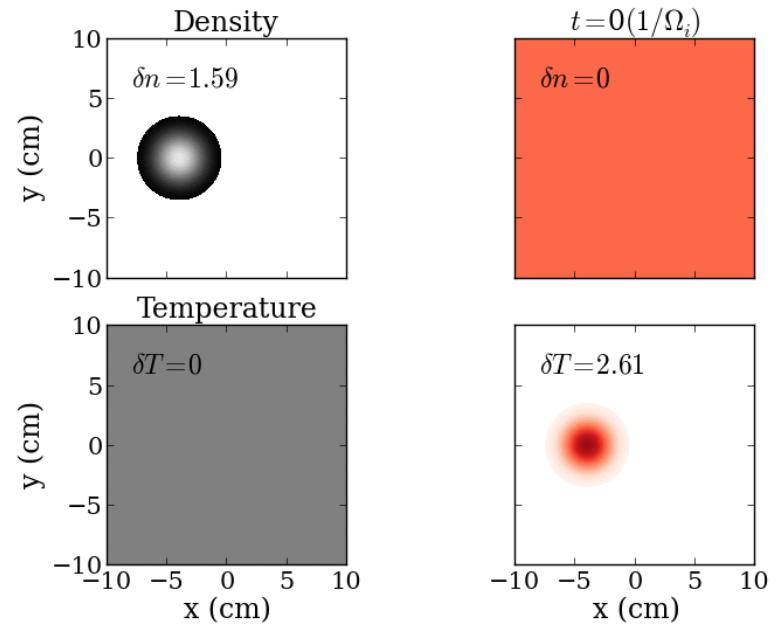
$$\delta T / T \gg \delta n / n$$

Localised near separatrix

Suggests a possible mechanism
 -> higher I_p leads to higher filament T_e and hence smaller V_r

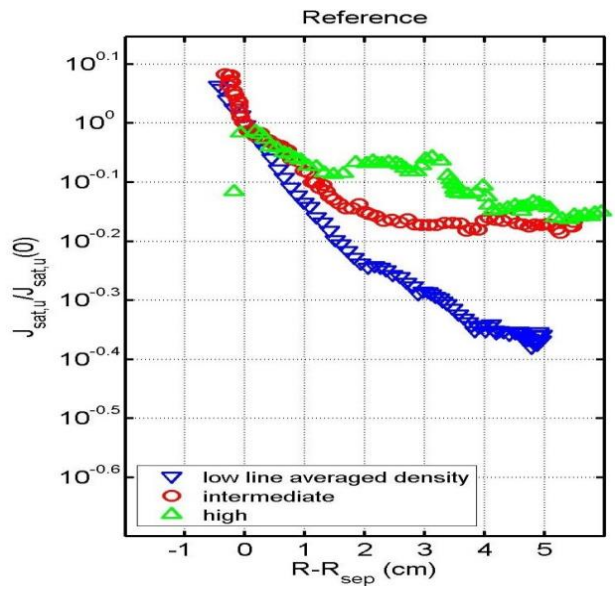
This effect is robust to changes in other parameters of the filament

[N.R.Walkden et al, Sub. PPCF]



- Flattening and broadening of SOL profiles observed with increasing the fuelling level.

Militello et al. NF 2016



EX/P4-31 F. Militello

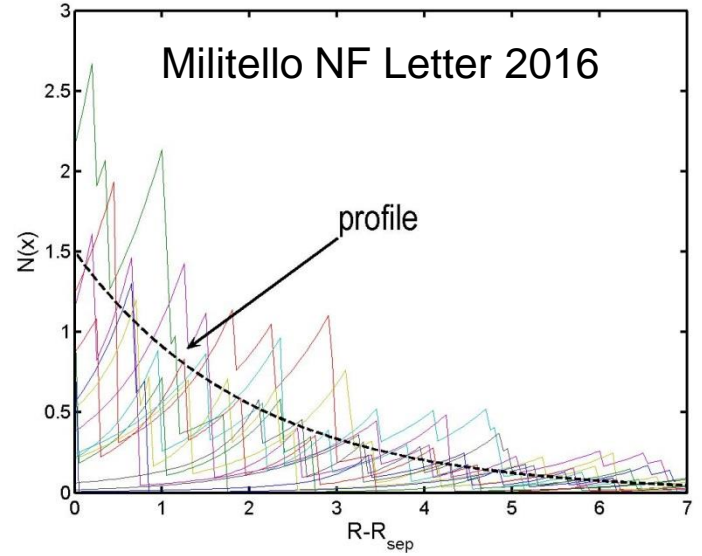
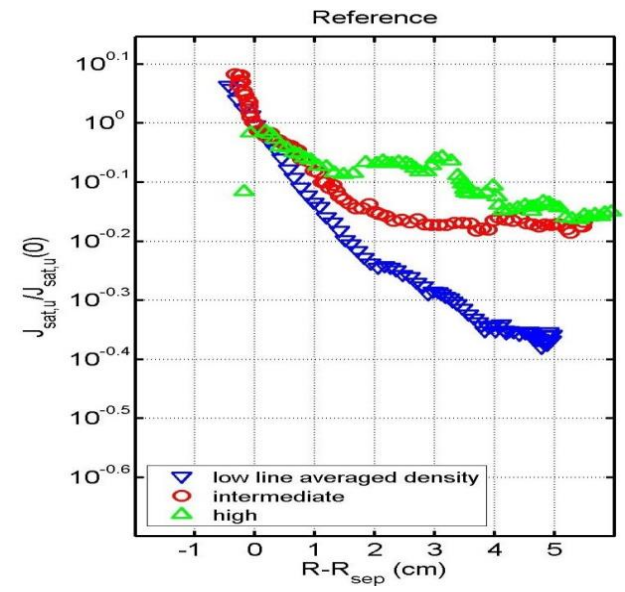
- Flattening and broadening of SOL profiles observed with increasing the fuelling level.
- A theoretical model was developed to interpret the relation between filament dynamics and features of the profiles.

$$N(x) = \frac{1}{\tau_w} \int_{-\infty}^{\infty} dt \int_0^{\infty} d\eta_0 \int_0^{\infty} dw [\eta(x, t) P_{\eta_0}(\eta_0) P_w(w)]$$

Profile

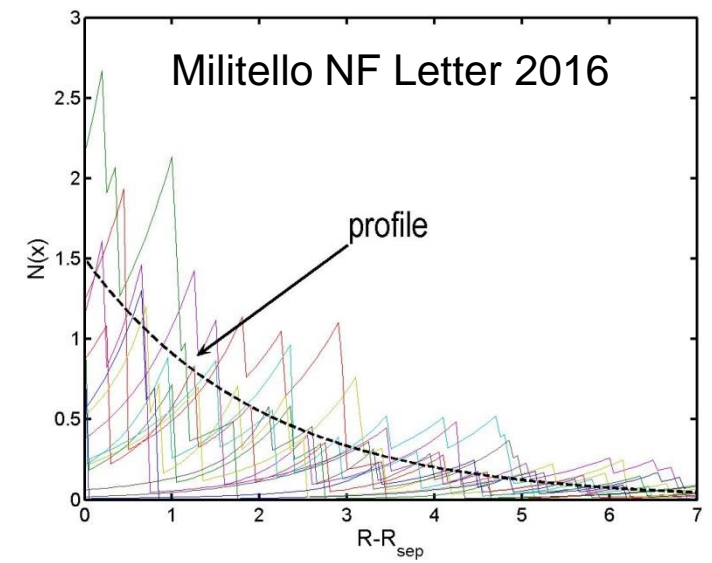
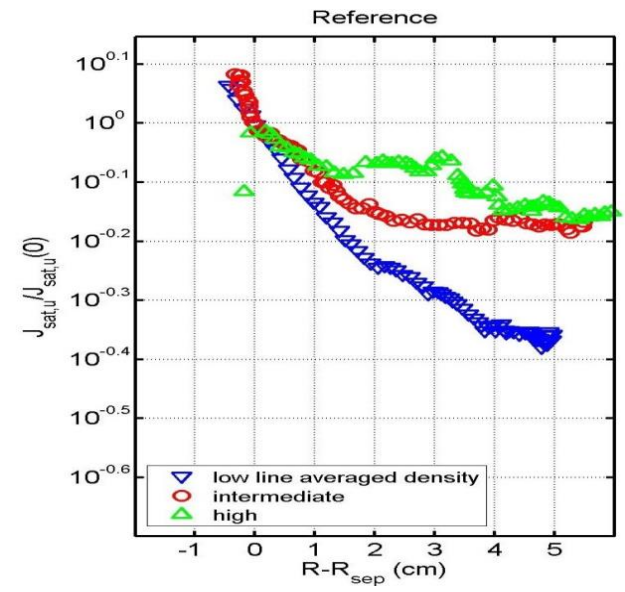
Filament shape and dynamics

Filaments statistics



EX/P4-31 F. Militello

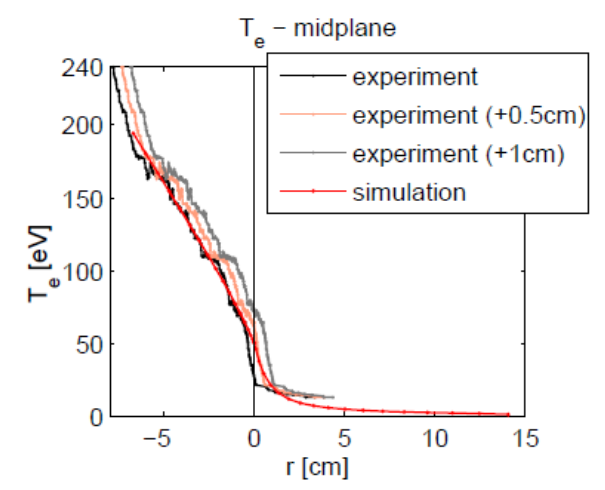
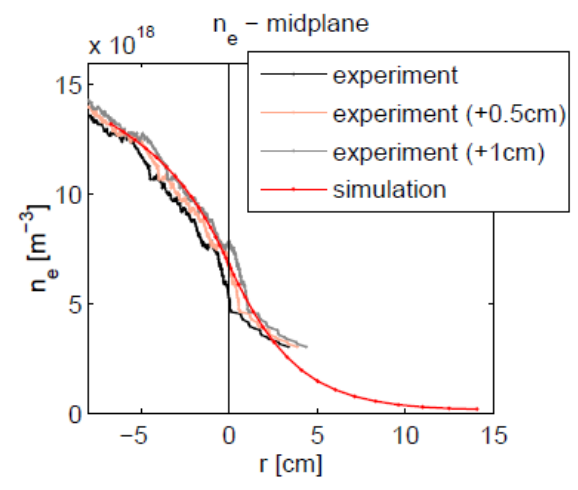
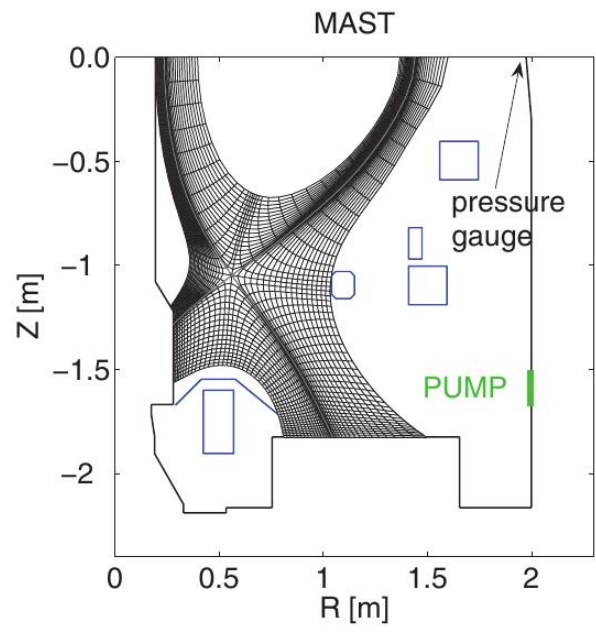
- Flattening and broadening of SOL profiles observed with increasing the fuelling level.
- A theoretical model was developed to interpret the relation between filament dynamics and features of the profiles.
- Shows that several effects can lead to the broadening including charge exchange and significant radial acceleration.



EX/P4-31 F. Militelto

SOLPS has been Benchmarked against L-mode shot 30356 in MAST

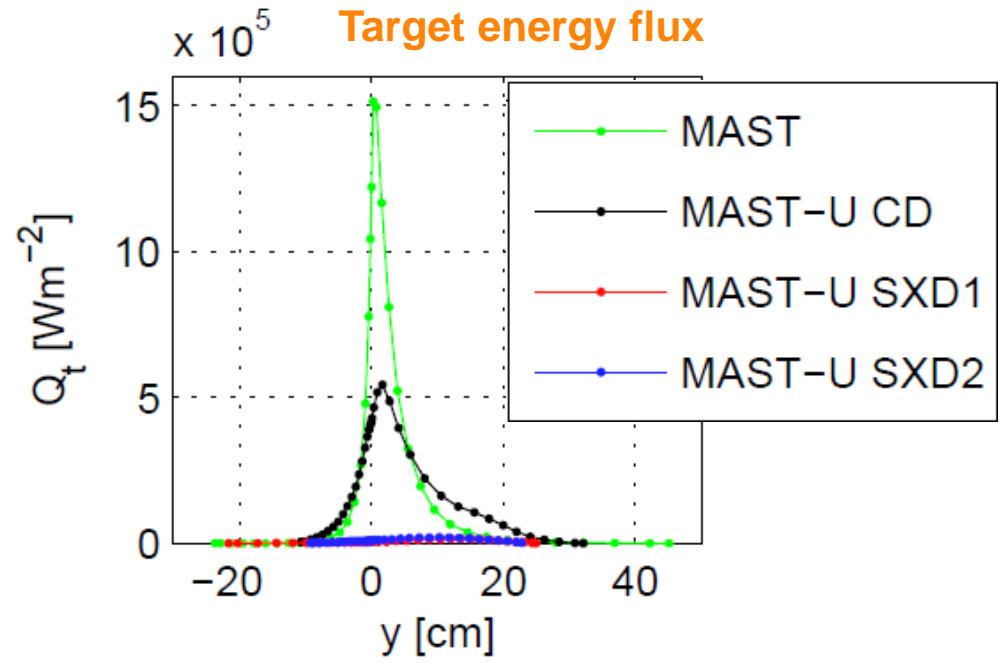
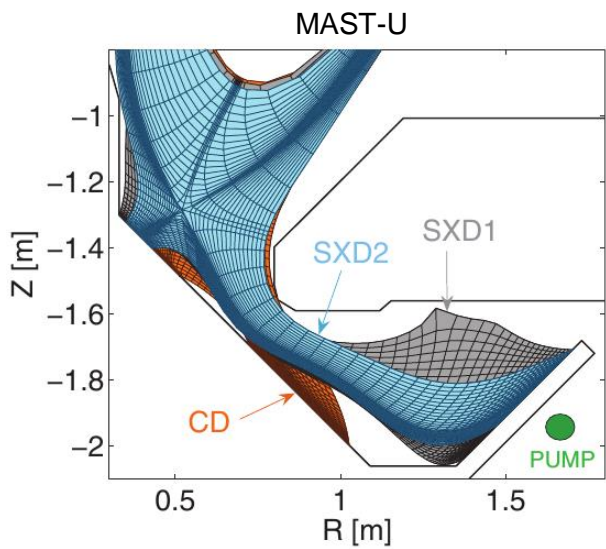
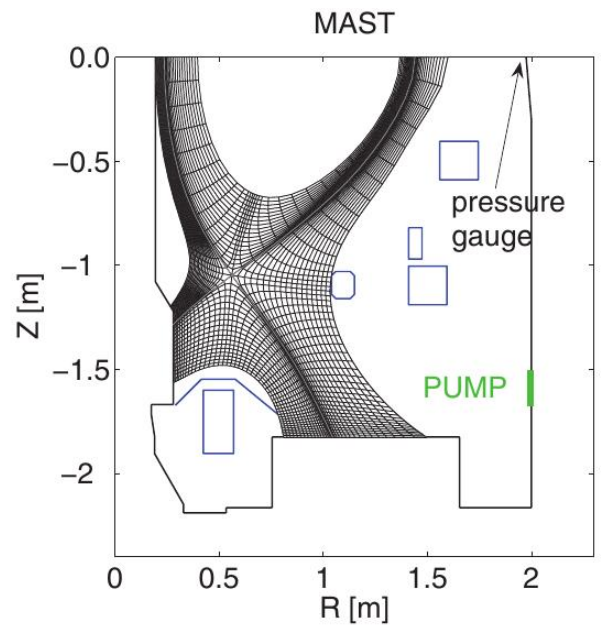
Extracted radial transport coefficients that well describe midplane and target data



Then used these to extrapolate to MAST-U

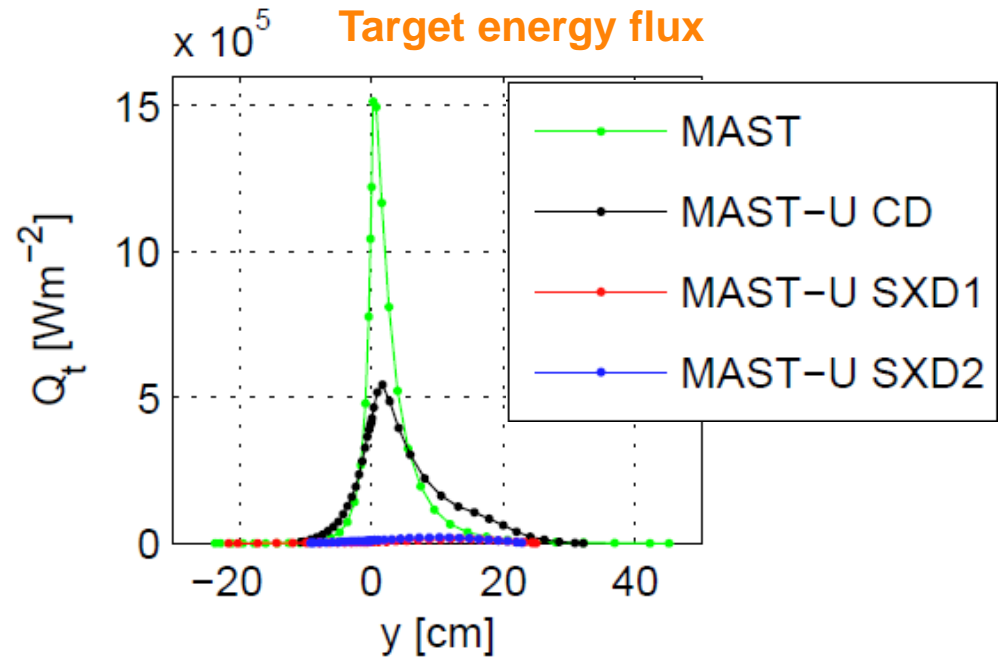
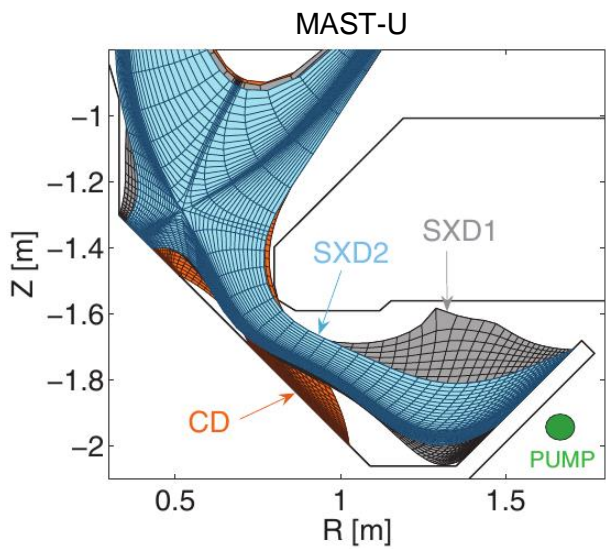
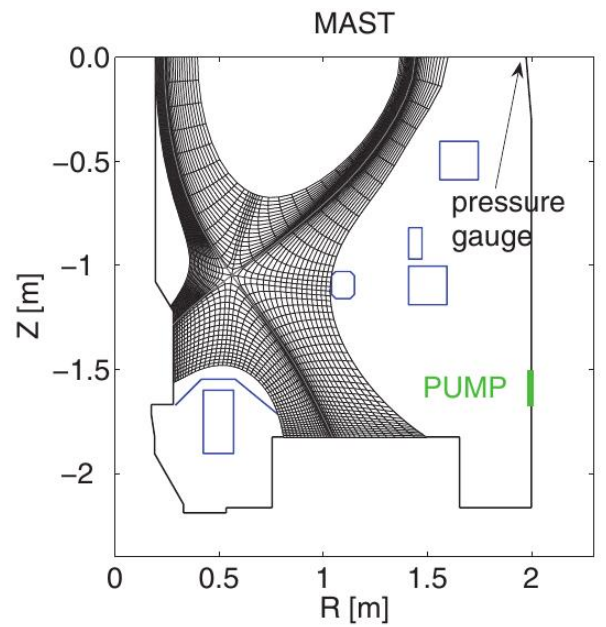
E. Havlíčková et al, PPCF 57 (2015) 115001

Super-X geometry pushes the target plasma into detachment, reducing the heat flux density and temperature at the target to ~zero.



E. Havlíčková et al, PPCF 57 (2015) 115001

Super-X geometry pushes the target plasma into detachment, reducing the heat flux density and temperature at the target to ~zero.



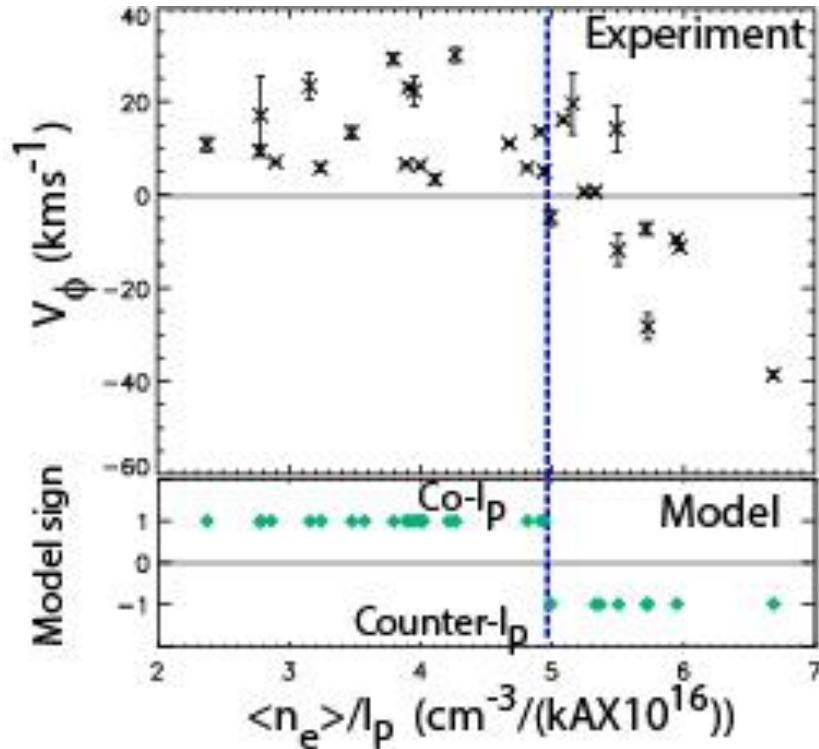
Attached regime in SXD in L-mode can be achieved if **the heating power** or the **pumping speed** is increased at the same density.

E. Havlíčková et al, PPCF 57 (2015) 115001

SOL transport

Core transport

Measurements of intrinsic rotation using Doppler Back Scattering (DBS)

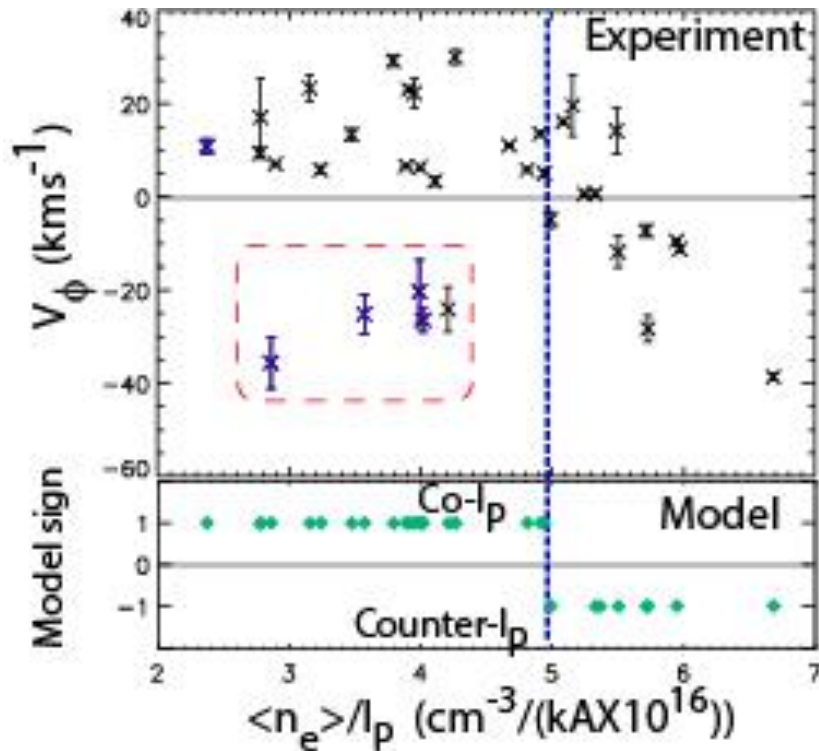


$\langle n_e \rangle / I_p \sim$ Collisionality

- Intrinsic toroidal rotation in MAST is large (up to $M_\phi \approx 0.2$) and depends on collisionality
- Experiment compared to model capturing effect of neoclassical flows on momentum transport
 - Barnes *Phys. Rev. Lett.* 111, 055005 (2013).
- Model correctly predicts sign in many cases, but....

Hillesheim, *Nucl. Fusion* 55, 032003 (2015).

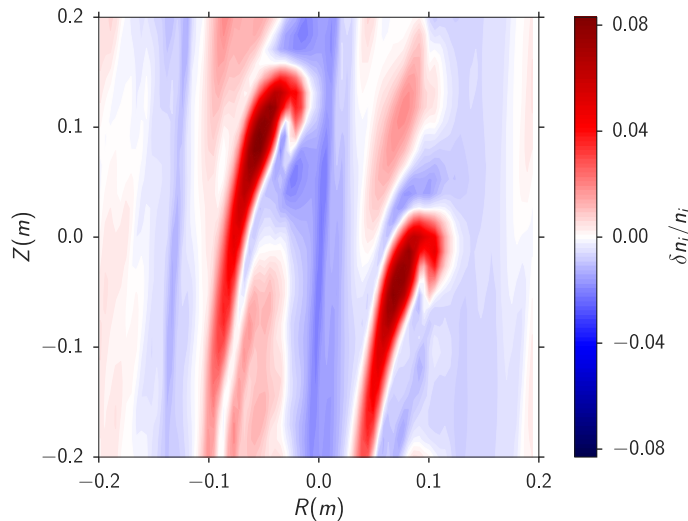
Measurements of intrinsic rotation using Doppler Back Scattering (DBS)



$\langle n_e \rangle / I_p \sim$ Collisionality

- Intrinsic toroidal rotation in MAST is large (up to $M_\phi \approx 0.2$) and depends on collisionality
- Experiment compared to model capturing effect of neoclassical flows on momentum transport
 - Barnes Phys. Rev. Lett. 111, 055005 (2013).
- Model correctly predicts sign in many cases, but there are some examples at low $\langle n_e \rangle$, low I_p that clearly disagree which indicate there may be additional physics at play

Hillesheim, Nucl. Fusion 55, 032003 (2015).



Ion scale turbulence $k_{\perp} \rho_i < 1.0$ is largely suppressed in STs by flow shear

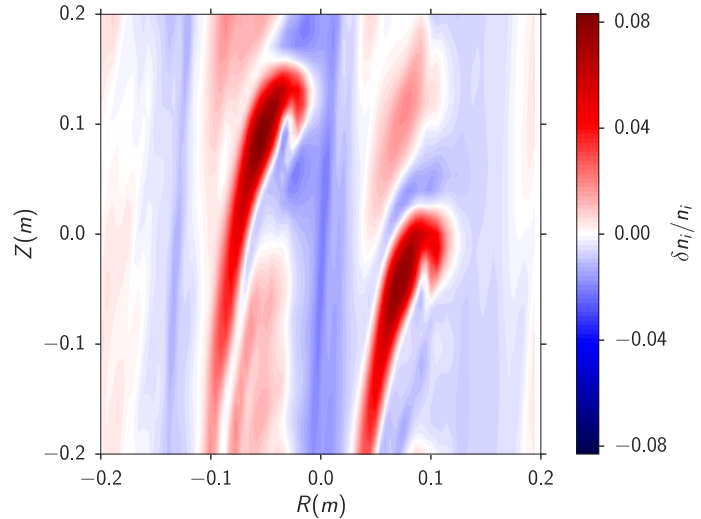
In the periphery of an L-mode plasma weak ion scale turbulence can exist

Local GS2 calculations at $\Psi_N \sim 0.7$ show that the experimental point is linearly stable

Non-linear simulations show that sub-critical turbulence can exist

For this sub-critical turbulence the heat flux is carried by a small number of long lived isolated structures

F. van Wyk Submitted to Nature

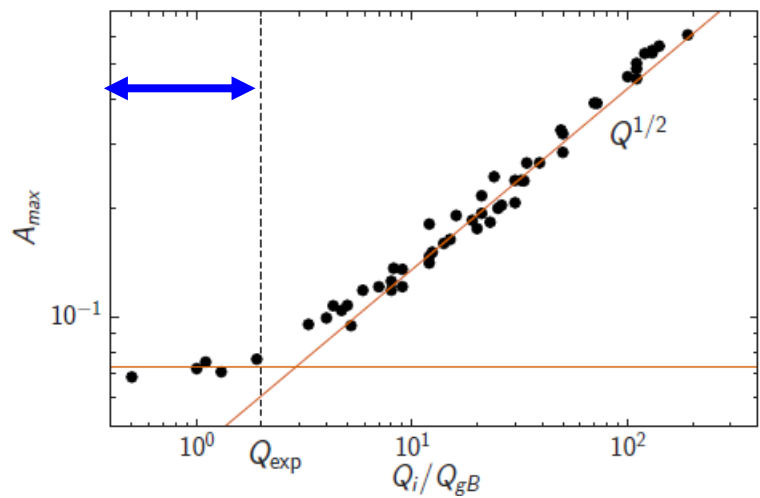


Close to “marginality” the **heat flux increases with the number of structures** rather than their amplitude increasing

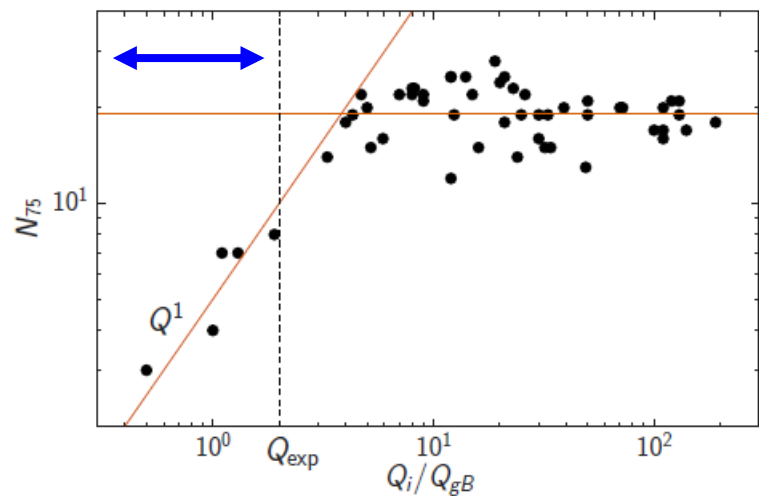
$$Q/Q_{gB} \sim N$$

Further from marginality the heat flux increases as A^2 while the N remains constant

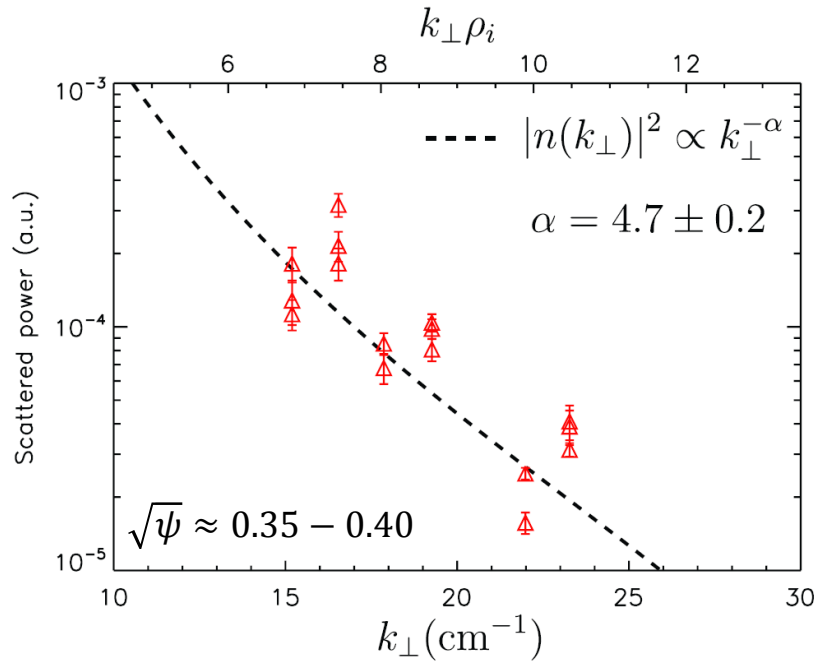
Marginal **Strongly Driven**



Marginal **Strongly Driven**

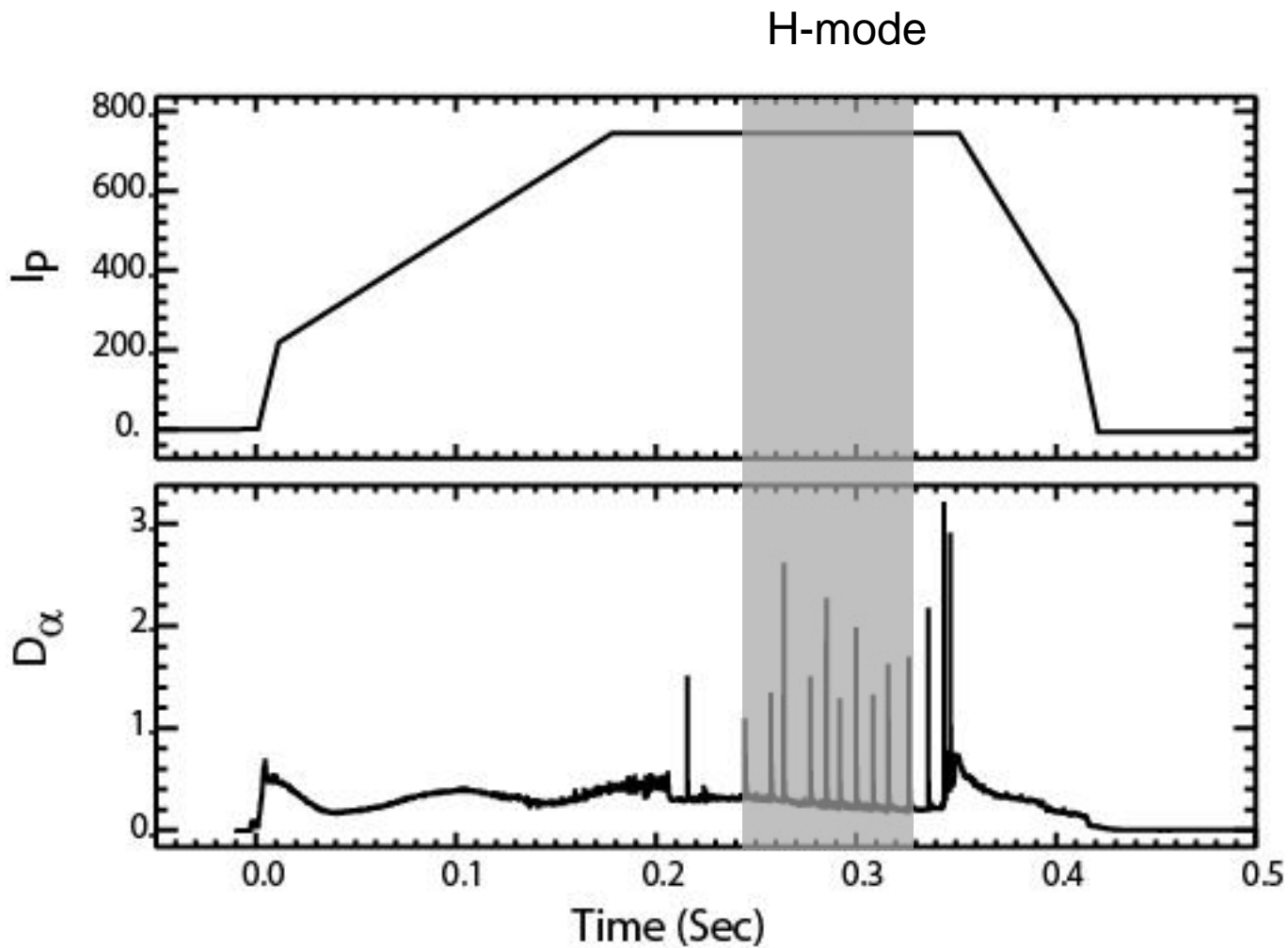


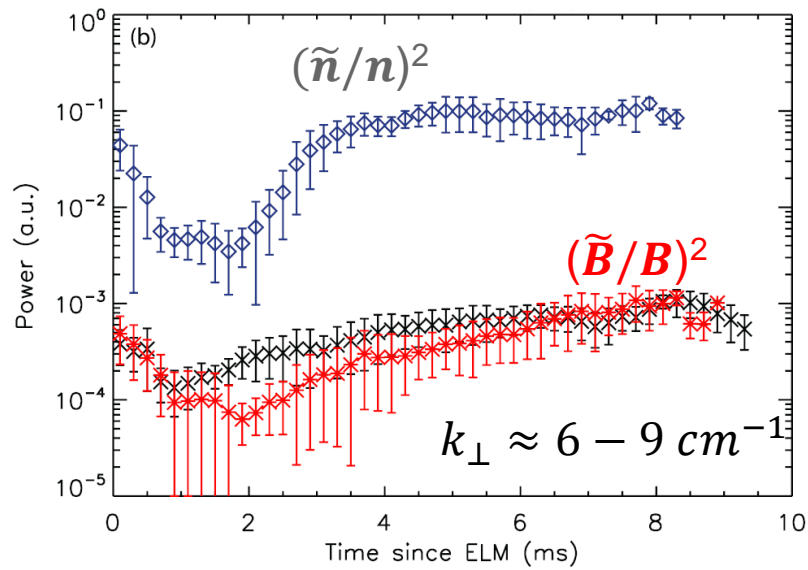
F. van Wyk Submitted to Nature



- Since Ion scale turbulence is largely suppressed in STs it is important to diagnose **higher wavenumber turbulence**
- A 2D beam steering of a Doppler Back Scattering system has been implemented to enable **high- k_{\perp}** measurements in the core
- A power law decrease in fluctuations is observed consistent with a turbulent kinetic cascade

Hillesheim, Nucl. Fusion 55, 073024 (2015).



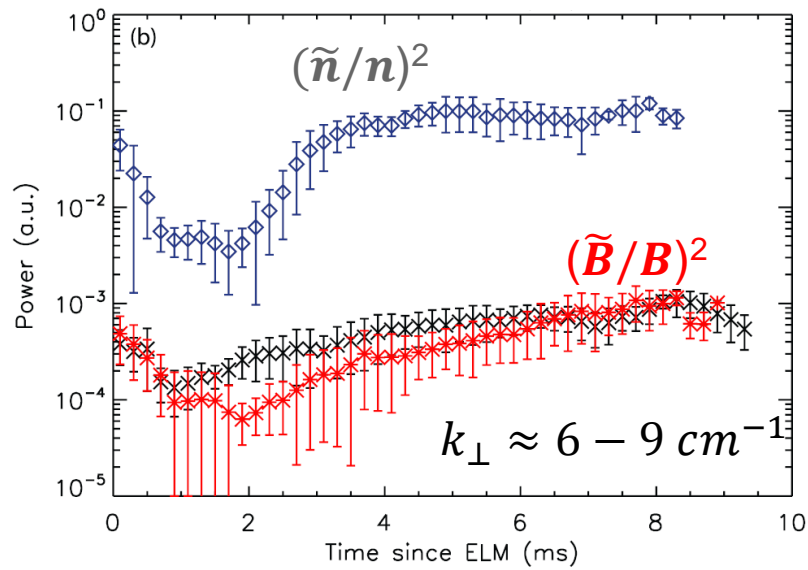


DBS used to measure density fluctuations $(\tilde{n}/n)^2$

Cross-polarization DBS used to measure the local magnetic field fluctuations $(\tilde{B}/B)^2$

At pedestal top dominant fluctuations at $k_{\perp} \sim 6-9 \text{ cm}^{-1}$

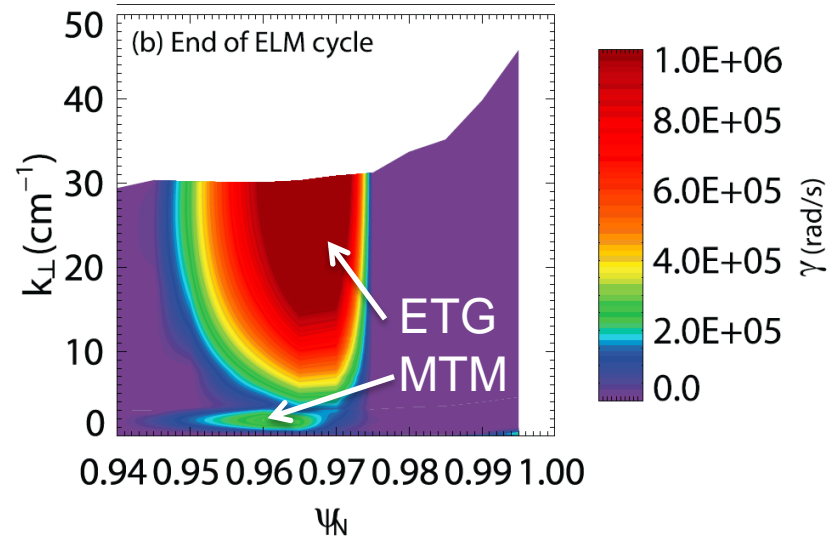
Hillesheim, *Plasma Phys. Controlled Fusion* 58, 014020 (2015)



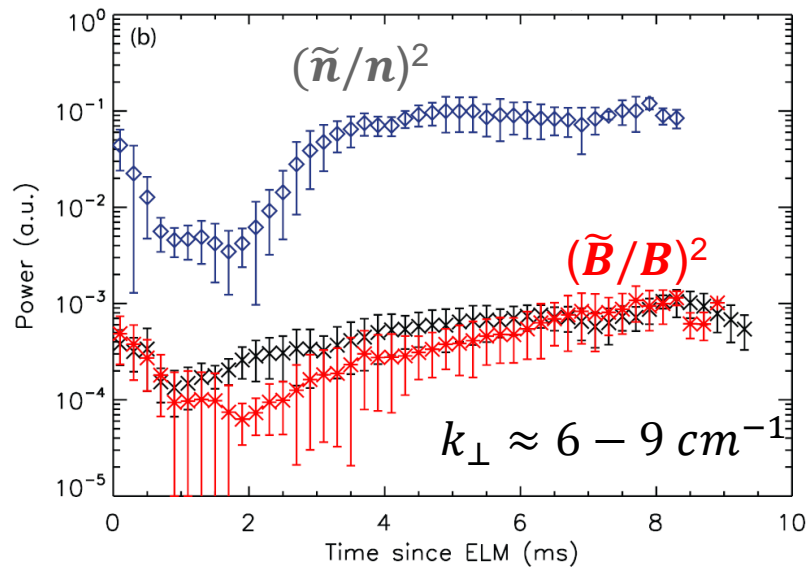
DBS used to measure density fluctuations $(\tilde{n}/n)^2$
 Cross-polarization DBS used to measure the local magnetic field fluctuations $(\tilde{B}/B)^2$

At pedestal top dominant fluctuations at $k_{\perp} \sim 6-9 \text{ cm}^{-1}$

Hillesheim, Plasma Phys. Controlled Fusion 58, 014020 (2015)



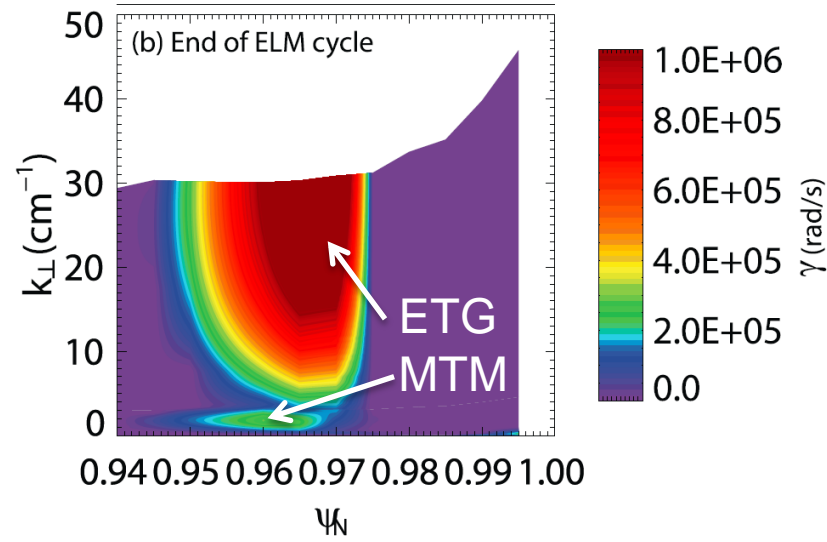
GS2 calculations show that both MTM and ETG are unstable at pedestal top



DBS used to measure density fluctuations $(\tilde{n}/n)^2$
 Cross-polarization DBS used to measure the local magnetic field fluctuations $(\tilde{B}/B)^2$

At pedestal top dominant fluctuations at $k_{\perp} \sim 6-9 \text{ cm}^{-1}$

Hillesheim, Plasma Phys. Controlled Fusion 58, 014020 (2015)

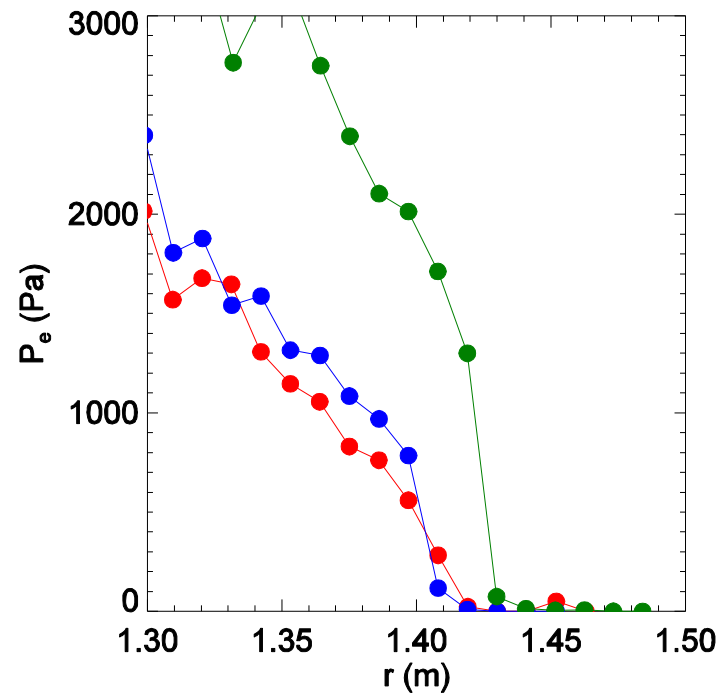
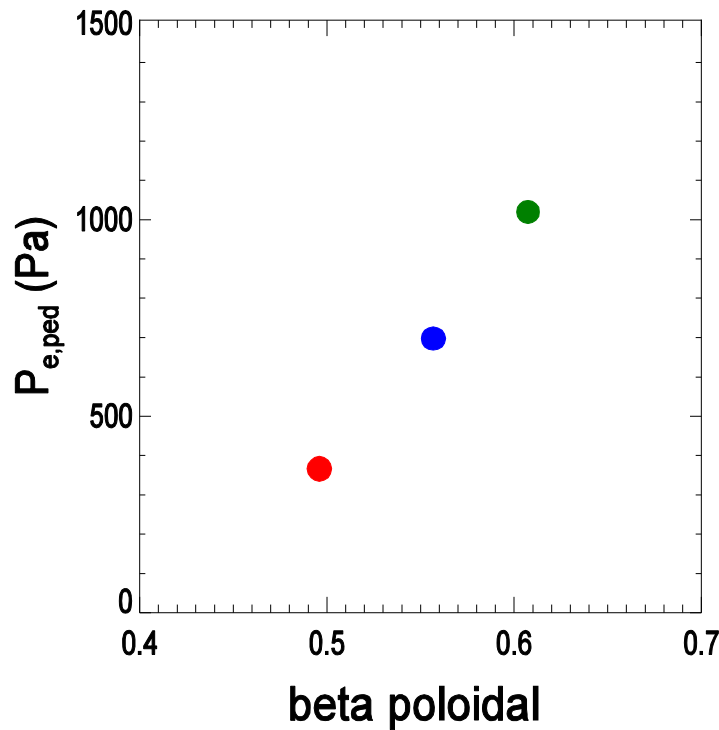


	k_{\perp} (cm^{-1})	$(\tilde{B}/B)/(\tilde{n}/n)$
Experiment	6-9	0.05
MTM	0.5-4	0.4
ETG	4-30	0.02

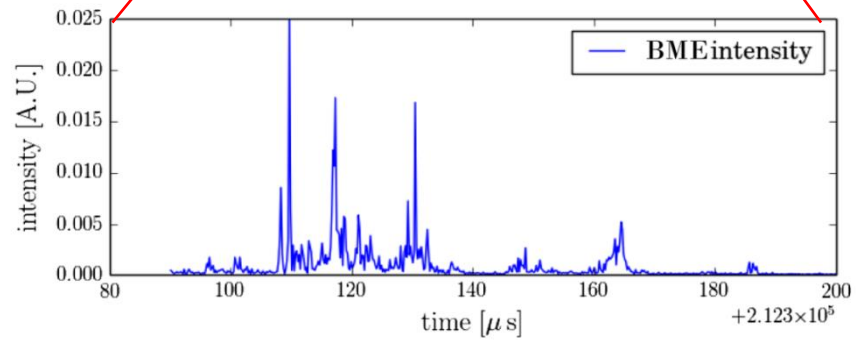
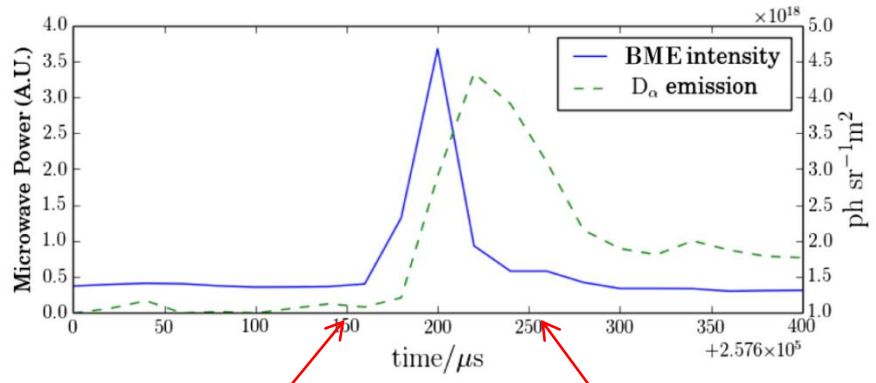
Consistent with ETG at pedestal top

Demonstration that core pressure affects the achievable pedestal height

- 36% increase in β core before the L-H transition produces a doubling of the pedestal height achievable before the first ELM



EX/3-6 I. Chapman



The Synthetic Aperture Microwave Imaging diagnostic (SAMI) has observed bursts of microwave emission during ELMs

Each burst has a duration of a $\sim 1\mu\text{s}$ and they exist during rise of $D\alpha$ emission

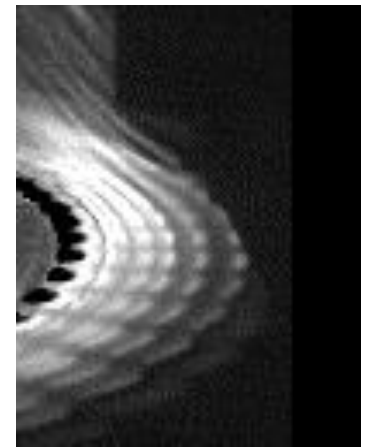
Modelling suggests that the bursts are due to the generation of non-thermal electrons [via an anomalous Doppler instability with the acceleration site very close to the plasma edge]

-> Possible evidence of a reconnection process occurring during the ELM

Freethy et al. Phys. Rev. Lett. **114** (2015) 125004

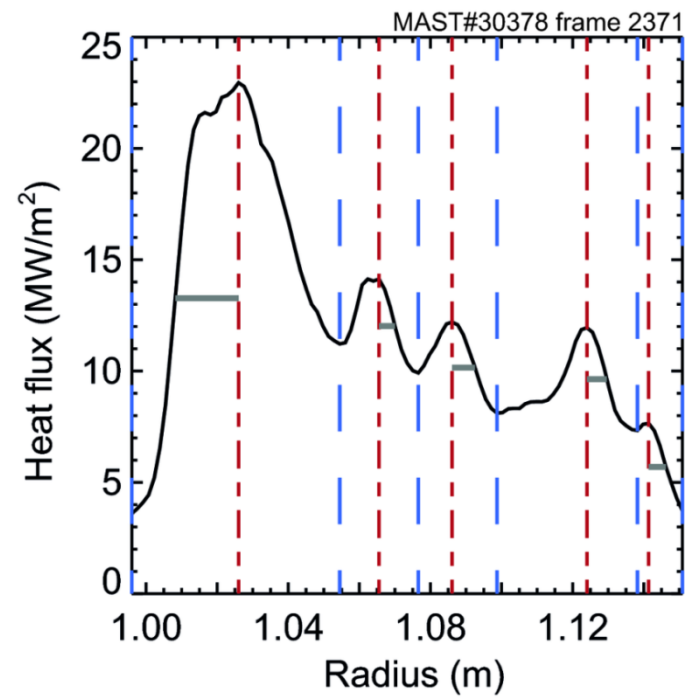
ELM filaments generate striations at the divertor

- lead to peaks in the heat flux profile that can be detected



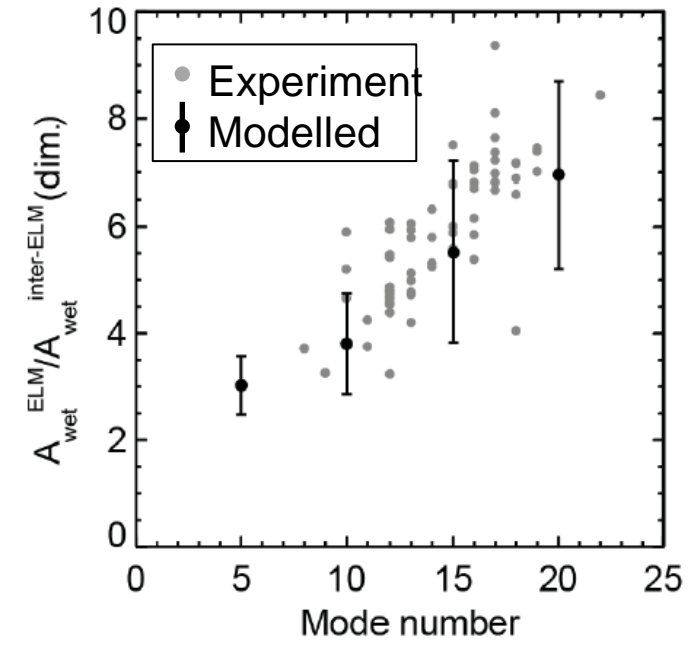
- The number and size of these filaments affect the wetted area

$$A_{wet} = \frac{2\pi \int q(r) r dr}{q_{peak}} = \frac{P_{tot}}{q_{peak}}$$



Wetted area increases with increasing mode number of ELM

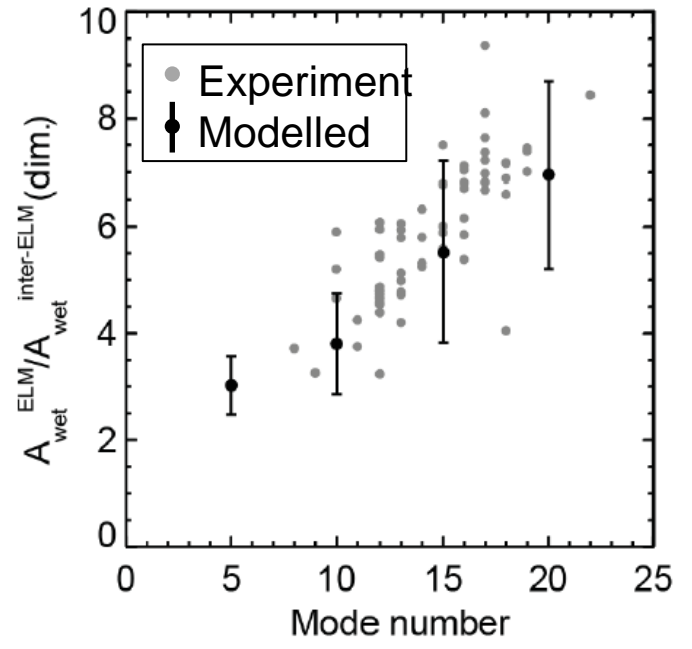
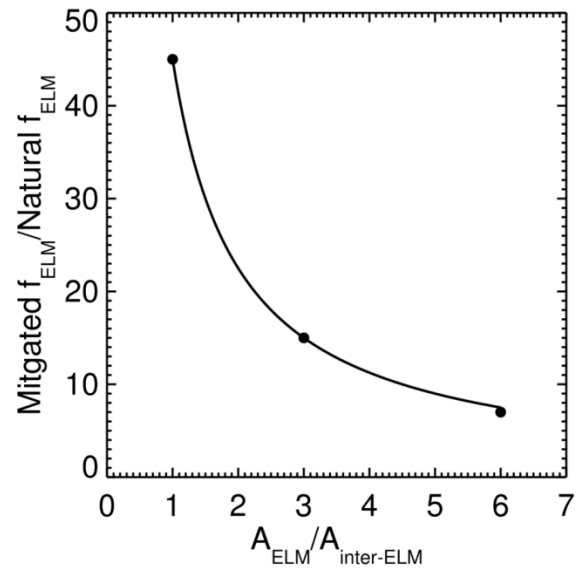
A Thornton et al. PPCF 2016



Wetted area increases with increasing mode number of ELM

A Thornton et al. PPCF 2016

ITER $I_p = 15$ MA



Level of ELM control required on ITER will depend on toroidal mode number of natural ELMs



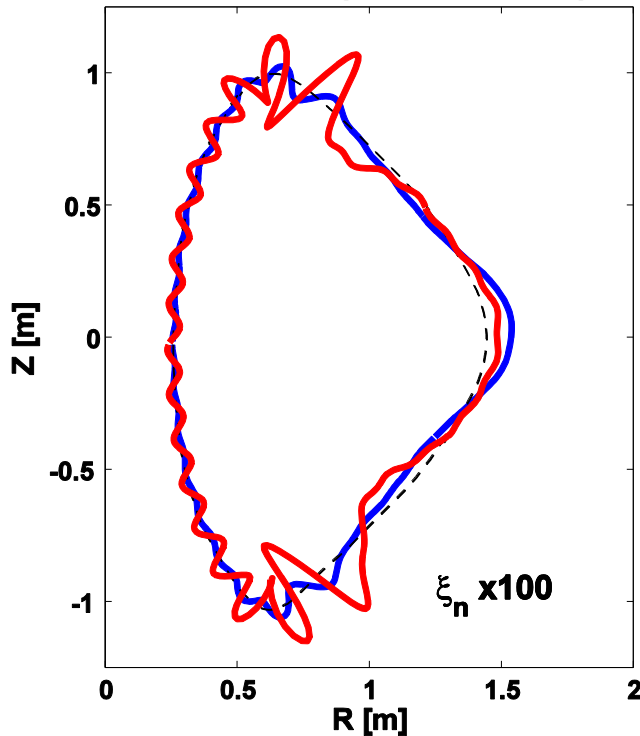
To reproduce observed filament behaviour in ELMs need to take into account the non-linear coupling of different toroidal mode numbers

TH/8-2 S. Pamela

ELM control using RMPs

Plasma displacement

The RMP field causes a 3D distortion of the plasma surface due to the plasma response to the applied field



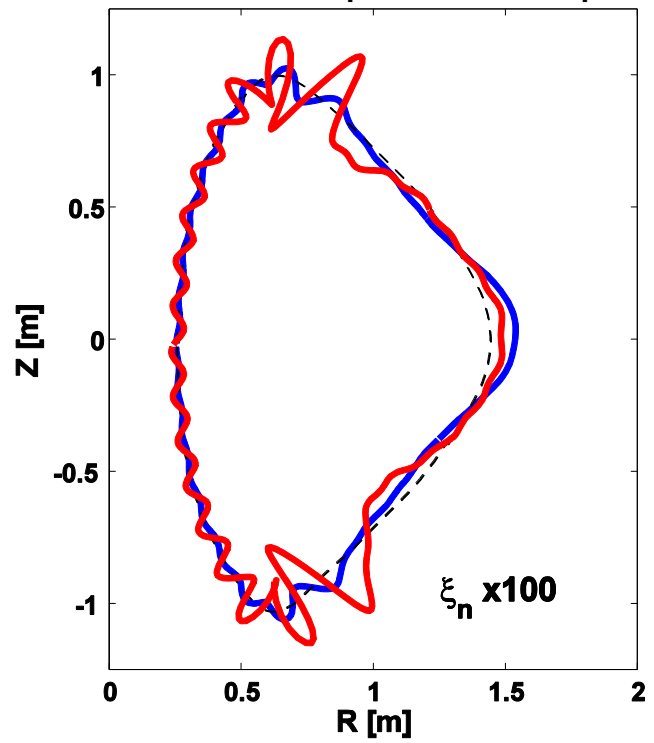
A core kink response leads to a peaking of the displacement near the midplane

An edge peeling response leads to a peaking of the displacement near the X-point

YQ Liu et al. NF 51 (2011) 083002

Plasma displacement

The RMP field causes a 3D distortion of the plasma surface due to the plasma response to the applied field

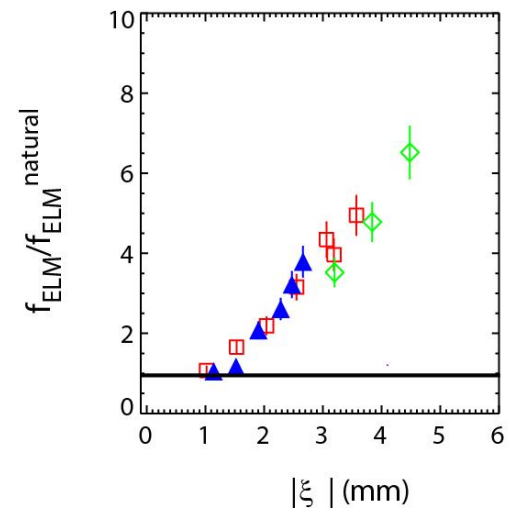


A core kink response leads to a peaking of the displacement near the midplane

An edge peeling response leads to a peaking of the displacement near the X-point

YQ Liu et al. NF 51 (2011) 083002

□ n=4 (SND) ▲ n=6 (SND) ◇ n=3 (SND)



Increase in ELM frequency correlated with size of X-point displacement – appears to be threshold at ~ 1.5 mm

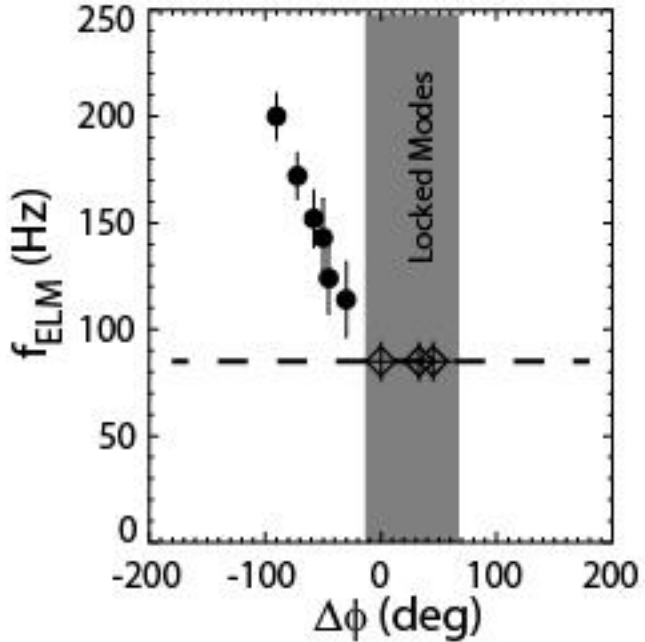
But is this the only criteria?

Alignment of applied field

$\Delta\phi$ scan used to adjust the alignment of the perturbation while keeping the plasma constant $\Delta\phi = -90^\circ$

f_{ELM} measured in repeat shots

1	2	3	4	5	6	7	8	9	10	11	12
+		-		+		-		+		-	
	+		-		+		-		+		-

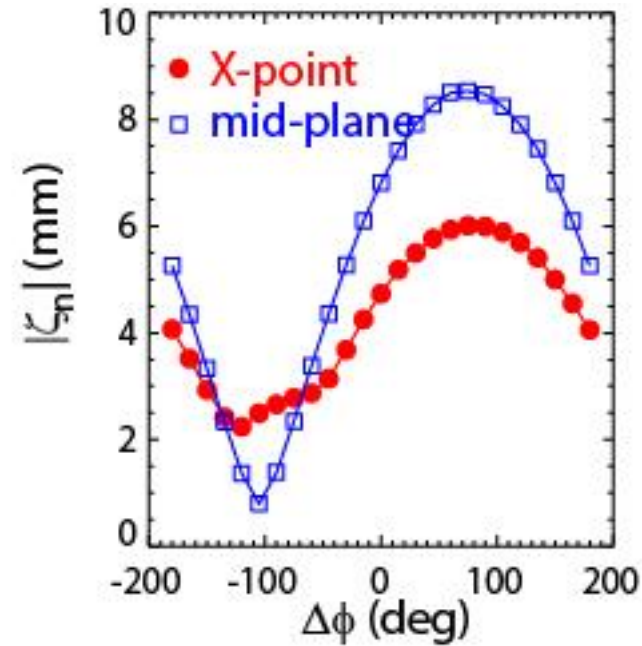
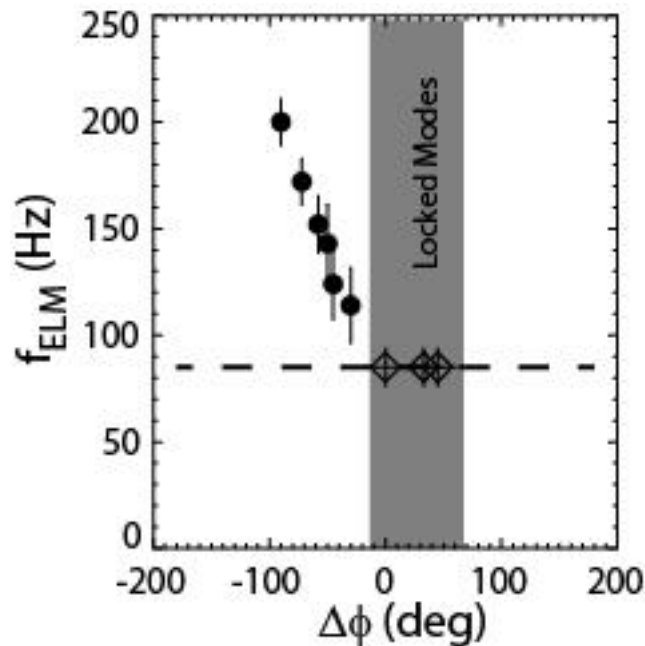


ELM mitigation only occurs in a narrow window of $\Delta\phi$

Plasma displacement

MARS-F plasma response calculations show that ELM mitigation only occurs where the X-point peaking is greater than the mid-plane peaking

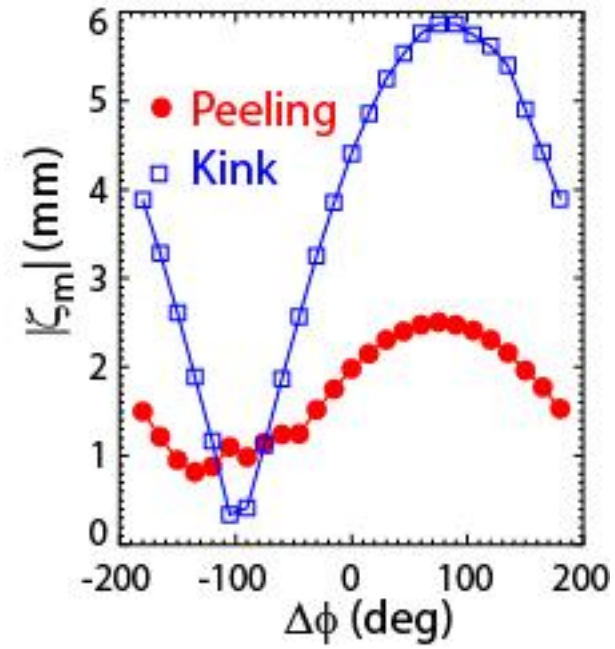
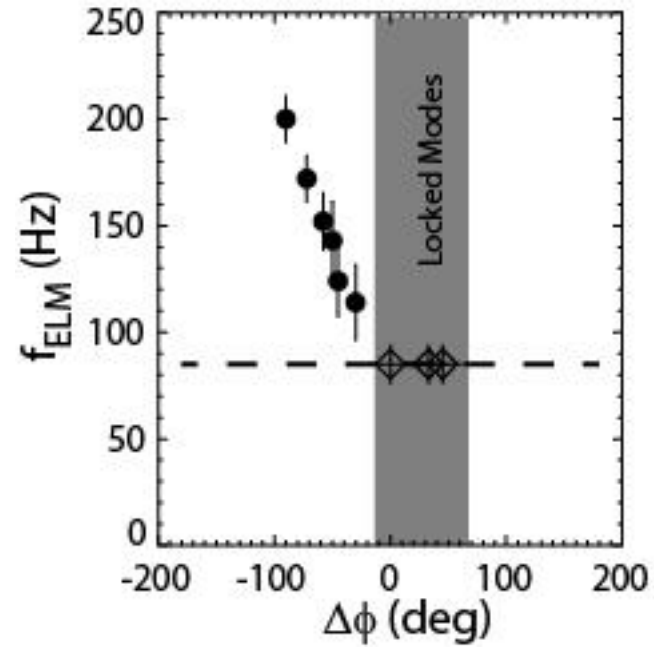
– not necessarily where the X-point peaking is largest



Alignment of applied field

Outside this window the core kink response is so large it causes locked modes

Access criteria: Optimise Peeling response while minimising the kink response



Although MAST has not operated since the last IAEA there has been substantial analysis and modelling performed on the data obtained previously

The aim has been to validate models which can then be used to extrapolate to future devices including MAST-U

MAST-Upgrade nearing end of construction (“core scope”)

Increased TF

Improved confinement

New Solenoid

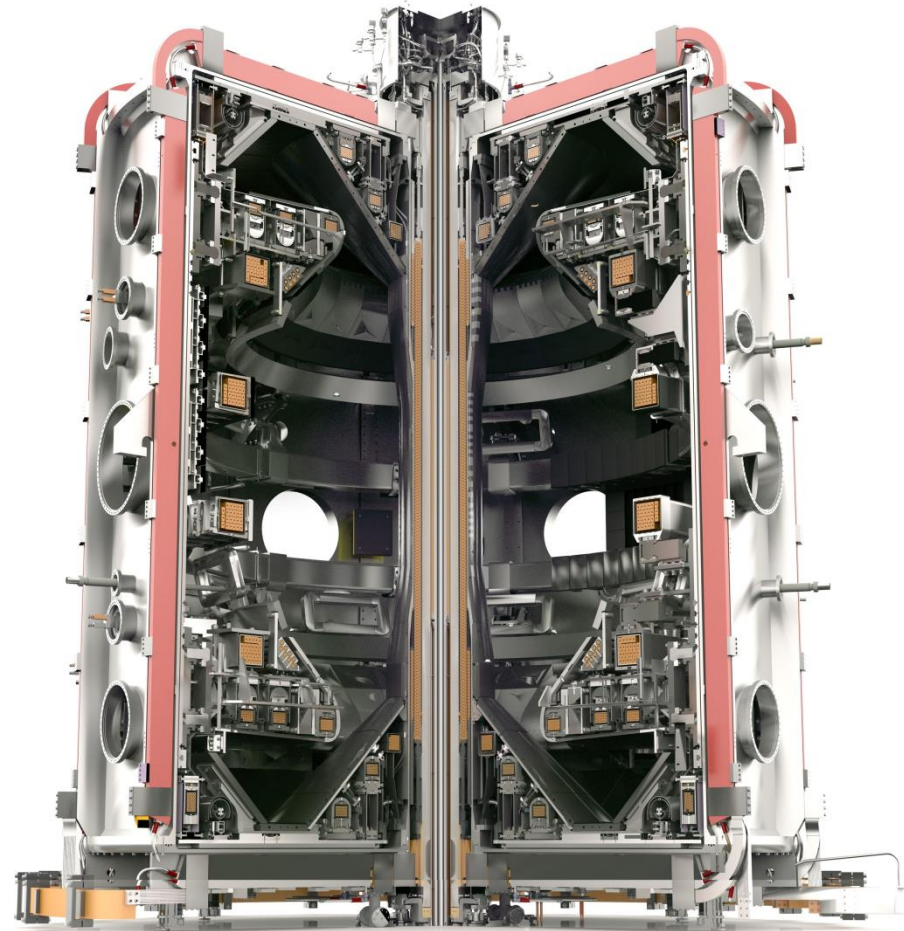
Greater I_p pulse duration

19 New PF Coils

Improved shaping

Off-Axis NBI

Improved profile control



Summary and future plans

MAST-Upgrade nearing end of construction (“core scope”)

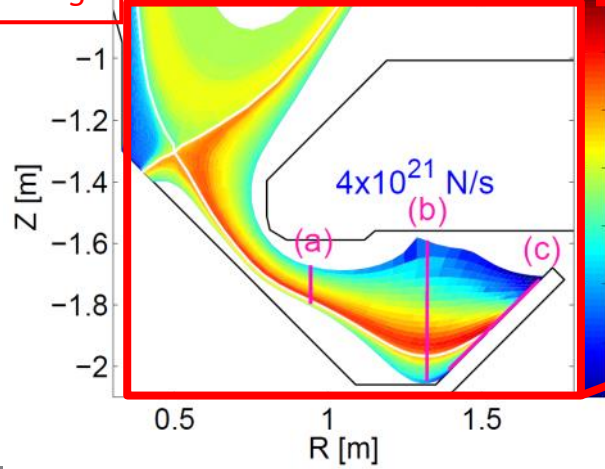
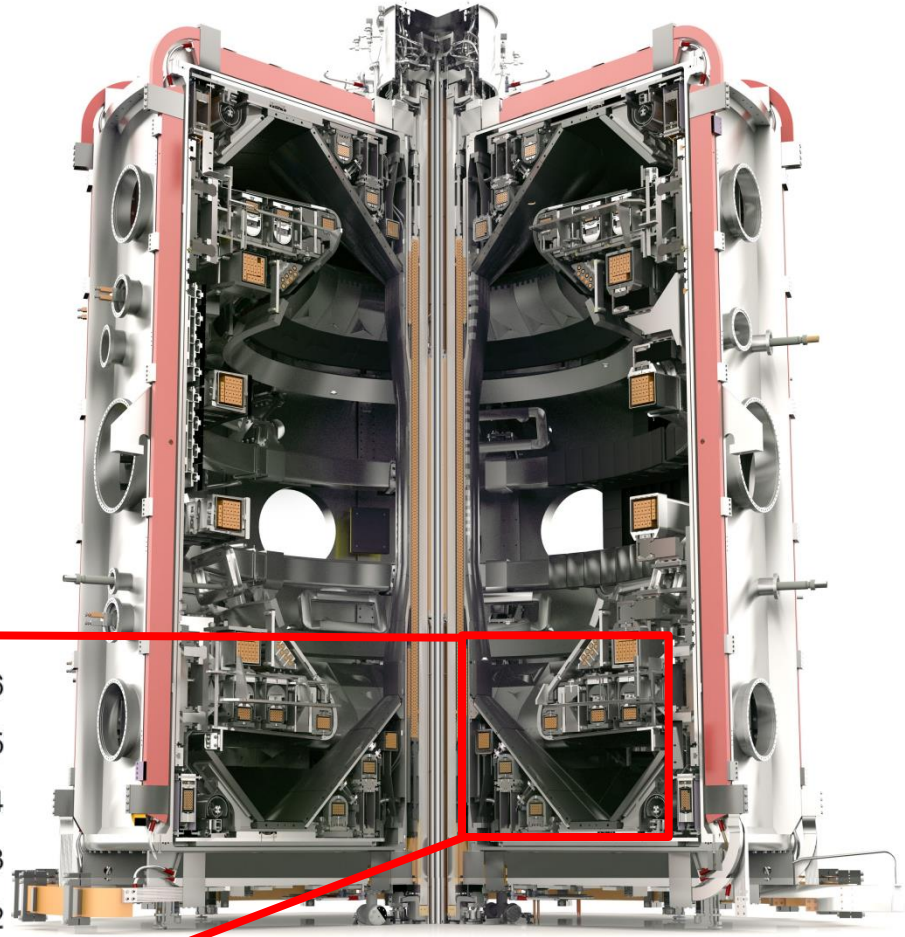
Increased TF
Improved confinement

New Solenoid
Greater I_p pulse duration

19 New PF Coils
Improved shaping

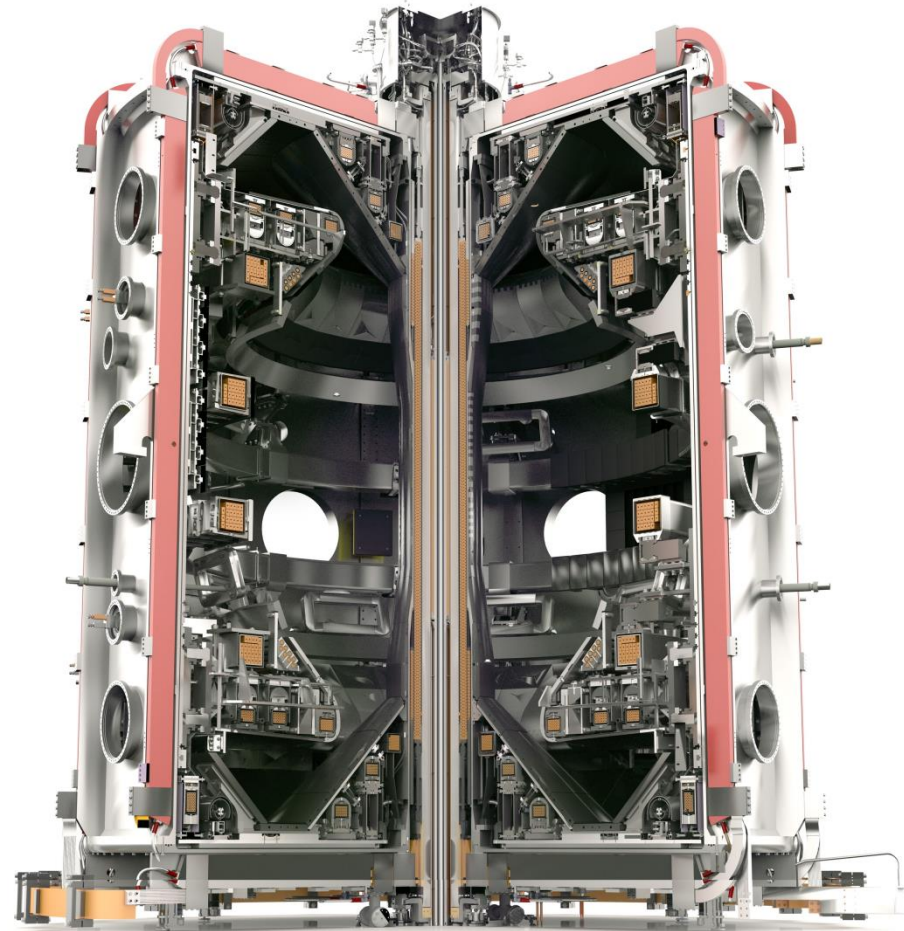
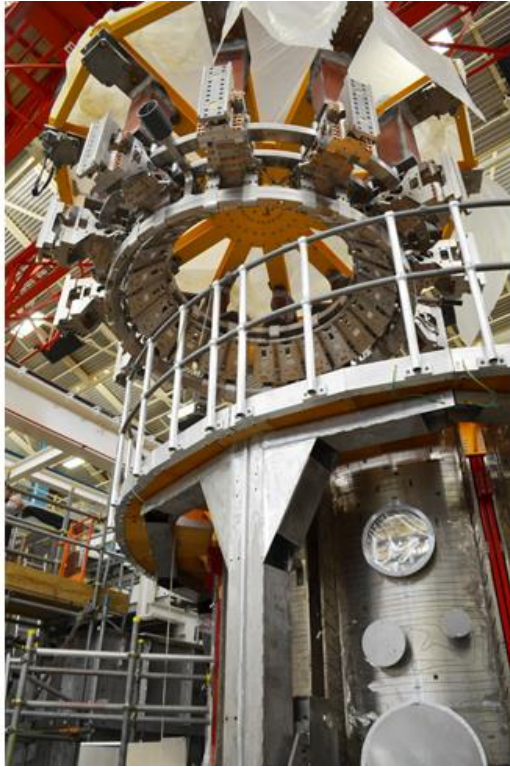
Off-Axis NBI
Improved profile control

Super-X Divertor
Improved power handling



Summary and future plans

MAST-Upgrade nearing end of construction (“core scope”)



Most of the Load assembly is now complete

MAST-Upgrade nearing end of construction (“core scope”)

We look forward to welcoming you to take part in the physics campaigns which will begin towards the end of 2017 when MAST-U will be operating as one of EUROfusion's Medium sized tokamaks

